Chapter 2
Adsorption of Dyes

Abstract Adsorption is one of the most commonly used, traditional separation technologies utilized for separation. Since it is an equilibrium-governed process, the process efficiency is excellent, but the throughput is relatively low. Nevertheless, because of its simplicity, this is one of the normally used technologies for dye removal from aqueous stream. Therefore, it is imperative to understand the modeling aspects of such adsorbent-based systems which is necessary for design and implementation of the technology. Additionally, the chapter describes the characteristics of the different commonly used adsorbents and its applicability.

Keywords Adsorbent • Chrysoidine • Eosin • Congo red • Activated charcoal

The word "adsorption" was formulated in 1881 by German physicist Heinrich Kayser to differentiate between the surface phenomena and intermolecular penetration. Adsorption can be divided into physical and chemical adsorption. Physical adsorption is controlled by the physical forces such as van der Waals forces, hydrophobicity, hydrogen bond, polarity, static interaction, dipole-dipole interaction, $\pi - \pi$ interaction, etc. When the species are adsorbed to the surface of the adsorbent by means of strong chemical interactions or bonding, it is referred to as chemisorption. The extent of adsorption depends on the nature of adsorbate such as molecular weight, molecular structure, molecular size, polarity, and solution concentration. It is also dependent on the surface properties of adsorbent such as particle size, porosity, surface area, surface charge, etc. The primary advantages of adsorption processes are:

1. Simple in design
2. Relatively safe and easy to operate
3. Inexpensive (compared to other separation processes)
4. Provides sludge-free cleaning operations (Gupta et al. 2000).

Selection of a suitable adsorbent is the primary concern for adopting adsorption in any process industries. The performance of the process is often limited by the equilibrium capacity of the adsorbent.

S. Mondal et al., *Advances in Dye Removal Technologies*, Green Chemistry and Sustainable Technology, DOI 10.1007/978-981-10-6293-3_2

2.1 Application of Adsorption in the Treatment of Process Wastewater

Various low-cost adsorbents for treatment of effluent containing heavy metals have been studied by various researchers in the past. Most of these adsorbents are prepared from the waste or by-products of other process plants or naturally occurring materials. A list of most commonly used low-cost adsorbents for heavy metal removal that is prepared from naturally occurring materials and processes are presented in Table 2.1.

2.2 Experimental Studies of Dye Adsorption

In the following sections, adsorption of chrysoidine, eosin, and Congo red by commercial activated carbon (CAC) has been presented.

2.2.1 Batch Adsorption

The batch adsorption is typically carried out in the solution phase containing dyes. The effects of agitation time and initial dye concentration on the percentage adsorption of dye by activated carbon at room temperature are shown in Figs. 2.1a, 2.1b, and 2.1c for chrysoidine, eosin, and Congo red. For all the cases, the percentage adsorption increases with agitation time for different initial dye concentration and attains equilibrium after some time.

Table 2.1 Low-cost high-capacity metal ion adsorbents

Metals	Adsorbent	Adsorption capacity (mg/g)	Reference
Zn^{2+}	Blast-furnace slag	103.3	83
	Powdered waste slag	168.0	147
Ni^{2+}	Red mud	160.0	112
Cu^{2+}	Blast-furnace slag	133.3	83
	Red mud	106.4	153
Cr^{6+}	Waste slurry	640.0	459
	Tea industry waste	455.0	165
Hg^{2+}	Waste slurry	560.0	159
Cd^{2+}	Fly ash	207.3	152
Pb^{2+}	Waste slurry	1030.0	159
V^{5+}	Waste metal sludge	24.8	97
As^{3+}, As^{5+}	Acid-activated laterite	24.5, 8.0	

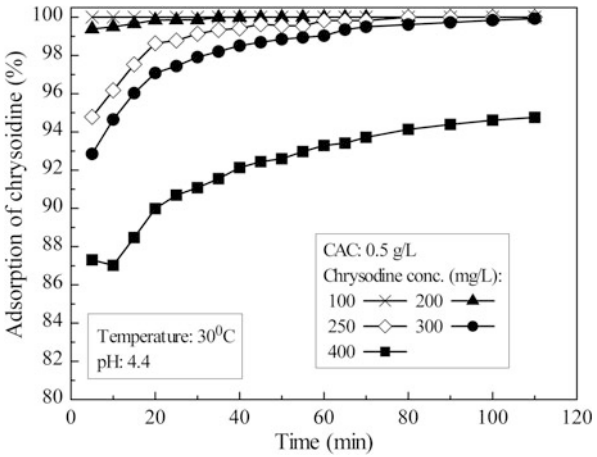

Fig. 2.1a Effects of agitation time and concentration of chrysoidine on percentage of adsorption (Reproduced from Purkait et al. (2004). With permission from Taylor & Francis Ltd)

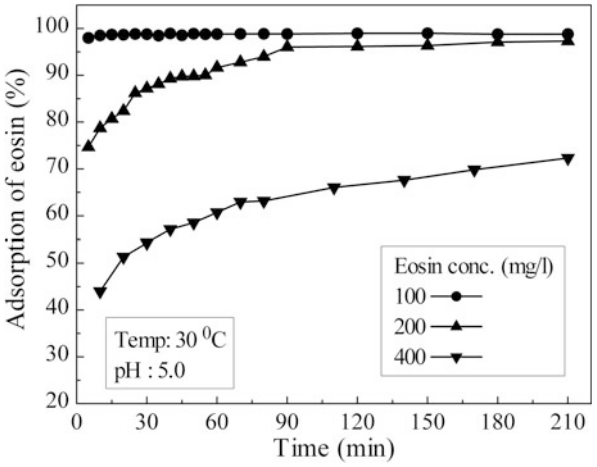

Fig. 2.1b Effects of agitation time and concentration of eosin on percentage of adsorption (Reproduced from Purkait et al. (2005). With permission from Elsevier)

From Fig. 2.1a, it may be observed that for all initial chrysoidine concentration, the percentage adsorption is found to be constant beyond 80 min. This indicates that equilibrium is attained at about 80 min for initial dye concentration in the range of 100–400 mg/L. It is also clear that the extent of adsorption depends on the initial dye concentration. For dye solution of lower initial concentration (up to 100 mg/L), the adsorption is very fast and almost 100% adsorption is achieved quickly. The dye adsorption at equilibrium decreases from 100% to about 94% as the dye concentration increases from 100 to 400 mg/L.

It is clear from Fig. 2.1b that up to an initial eosin concentration of 100 mg/L, more than 99% adsorption is achieved within 5 min. For an initial concentration of 200 mg/L, the percentage adsorption increases until 90 min and becomes constant thereafter. For a feed concentration of 400 mg/L, the percentage adsorption increases rapidly for about 90 min, and the increase becomes gradual thereafter.

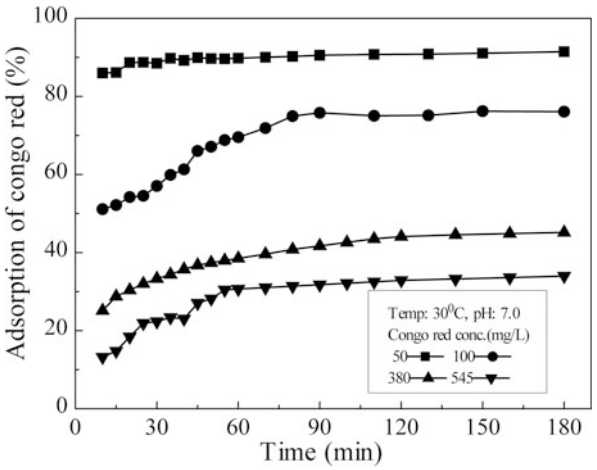

Fig. 2.1c Effects of agitation time and concentration of Congo red on percentage of adsorption (Reproduced from Purkait et al. (2007). With permission from Elsevier)

For 210 min of operation, the dye adsorption is 99.6% for an initial dye concentration of 100 mg/L but only 72.3% for 400 mg/L.

Figure 2.1c describes the variation of Congo red adsorption with time for different initial dye concentration. The percentage adsorption of Congo red is found to be constant beyond 50 min. This indicates that the equilibrium is attained within 50 min for the range of initial dye concentrations. It is also clear that the extent of adsorption depends on the initial dye concentration. For dye solution of lower initial concentration, the adsorption is very fast and 90% of adsorption is achieved quickly. The percentage dye adsorption at equilibrium decreases from 90% to 28% as the dye concentration increases from 50 to 545 mg/L.

The effects of adsorbent dose on the extent of chrysoidine adsorption are shown in Fig. 2.2 for initial dye concentrations of 700 mg/L. It is clear from the figure that percentage adsorption increases with time up to 80 min and also with adsorbent dose. Percentage adsorption increases from about 77 to 99% when the adsorbent dose increases from 0.75 to 1.40 g/L. This increase in percentage adsorption may be due to the fact that the number of available sites for adsorption increases with adsorbent dose.

The pH of the solution has significant influence in the rate of adsorption. The percentage dye adsorption at different pH is shown in Figs. 2.3a, 2.3b, and 2.3c for chrysoidine, eosin, and Congo red, respectively. Figure 2.3a describes the variation of chrysoidine adsorption at different pH for an initial dye concentration of 400 mg/L. The color of chrysoidine dye in aqueous medium is red (λ_{max}: 457 nm) in acidic pH but changes its color from red to yellow (λ_{max}: 442 nm) in basic pH. This is due to the presence of chromophore in the structure of chrysoidine. A chromophore is any structural feature (in this case, $-N = N-$) which produces light absorption in the ultraviolet region or color in the visible region. An auxochrome is any group (in this case $-NH_2$) which, although not a chromophore, leads to a red shift when attached to a chromophore. Thus, the combination of chromophore and auxochrome behaves as a new chromophore. Bathochromic effect (red shift) and

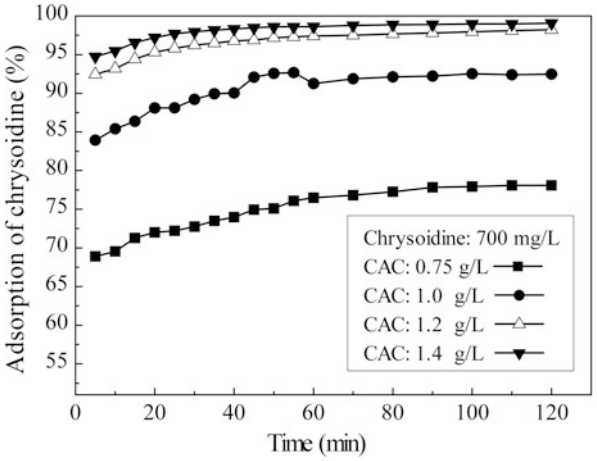

Fig. 2.2 Effects of agitation time and adsorbent dose on percentage adsorption (Reproduced from Purkait et al. (2004). With permission from Taylor & Francis Ltd)

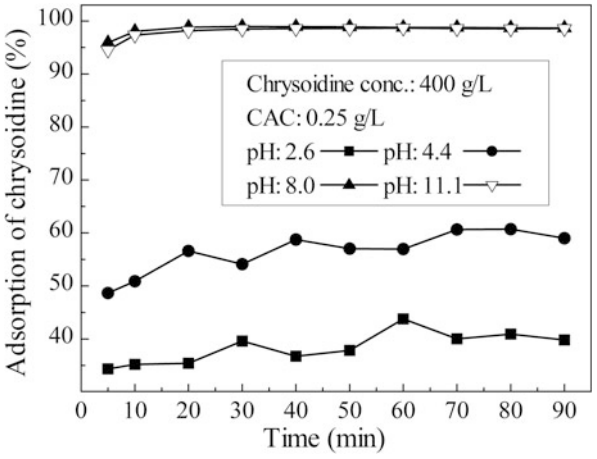

Fig. 2.3a Effect of initial pH on percentage of adsorption for 400 mg/L of feed chrysoidine (Reproduced from Purkait et al. (2004). With permission from Taylor & Francis Ltd)

hypsochromic effect (blue shift) are the shifting of the absorption band to the longer and shorter wavelengths (Finar 1973). Therefore, due to blue shift, chrysoidine changes its color in basic pH.

Adsorption followed by desorption technique is generally used to get the more concentrated form of the dye solution. One of the most common desorption technique is the pH treatment. But problem arises for the dyes which are highly pH sensitive, like chrysoidine as discussed in the previous paragraph.

Most of the activated carbon contains some oxygen complexes on the surface, e.g., (a) strongly carboxylic groups, (b) carbonyl groups, and (c) phenolic groups (Motoyuki 1990). These groups are nucleophilic in nature and potential adsorbing sites. In acidic pH, these active sites get blocked by hydrogen ion leading to reduction in adsorption. Hence, adsorption of chrysoidine on activated carbon is less in acidic pH. It is found from Fig. 2.3a that at pH 2.6, adsorption is nearly 62%

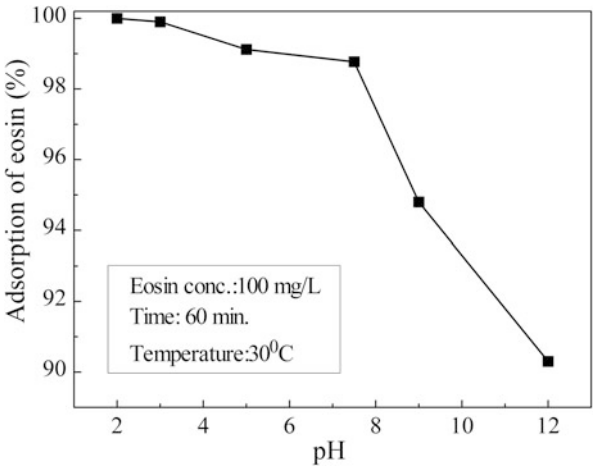

Fig. 2.3b Effect of pH on the percentage adsorption of feed eosin (Reproduced from Purkait et al. (2005). With permission from Elsevier)

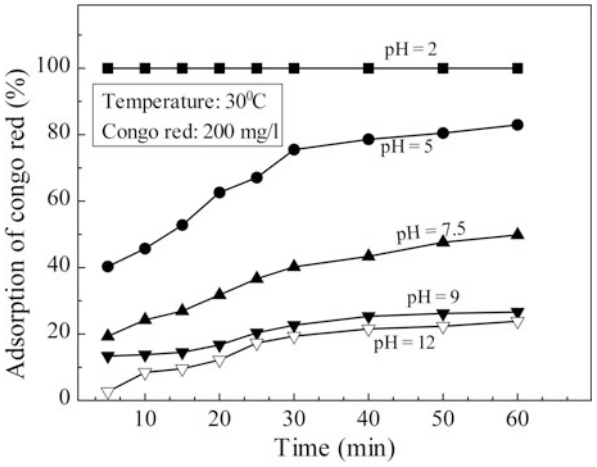

Fig. 2.3c Effect of initial pH on percentage of adsorption for 200 mg/L of feed Congo red (Reproduced from Purkait et al. (2007). With permission from Elsevier)

for the feed dye concentrations of 400 mg/L at the end of experiment. The percentage adsorption decreases from about 98 to 40%, when pH decreases from 11.1 to 2.6. From Fig. 2.3a, it may be observed that the adsorption of this dye is more at the basic pH.

The percentage of eosin adsorption at different pH levels are shown in Fig. 2.3b for an initial dye concentration of 100 mg/L. pH plays an important role on adsorption capacity by influencing the chemistry of both the dye molecule and the activated carbon in aqueous solution. Eosin is a dipolar molecule at low pH. Activated carbon contains oxygen complexes on its surface, e.g., strongly carboxylic groups, carbonyl groups, and phenolic groups (Motoyuki 1990). These groups are nucleophilic in nature. With decrease in pH of the dye solution, more dye molecules are protonated and get adsorbed on the surface of the activated carbon. It can be observed from Fig. 2.3b that at pH 2, adsorption is about 100% for an initial

dye concentration of 100 mg/L. Percentage adsorption decreases with increase in pH. For the initial dye concentration of 100 mg/L, the removal is 91% for a pH of 12.

The percentage of Congo red adsorption at different pH has been shown in Fig. 2.3c for the initial dye concentrations of 200 mg/L. The initial pH of dye solution plays an important role particularly on the adsorption capacity by influencing the chemistry of both dye molecule and activated carbon in aqueous solution. Congo red is a dipolar molecular at lower pH and exists as anionic form at higher pH as shown in Fig. 2.3c. The sodium and potassium salt of anionic Congo red in aqueous medium is red in color in basic pH up to 10. Above the pH value of 10, the degree of red color changes from the original one. It has also been found that as the pH decreases, the color of Congo red solution changes from red to dark blue. Therefore, the pH of the medium needs to be maintained between 5 and 10 to treat Congo red. These variations of color with pH suggest that the extent and nature of ionic character of Congo red molecule depend on the pH of the medium. The variations in the extent of adsorption of Congo red on activated carbon with pH are due to the difference in ionic character of the dye molecule. With decrease in pH of dye solution, more dye molecules are protonated and chemisorbed on the nucleophilic sites of the surface of CAC. It is found from the figure that at pH 2, adsorption is about 100%. On the other hand, the percentage adsorption decreases with increase in pH of the dye solution. This is because at higher pH, dye molecules exist in anionic form, and due to interionic repulsion, less adsorption takes place. For the feed dye concentration of 200 mg/L, the percentage adsorption decreases to 25% at the end of the experiment when the pH is 12. From Fig. 2.3c, it may be observed that the adsorption of Congo red is maximum at the acidic pH. Therefore, when Congo red is present in the solution as red color, the operating pH for maximum adsorption should be kept at 5.

Effects of temperature on the extent of adsorption are shown in Figs. 2.4a, 2.4b, and 2.4c for chrysoidine, eosin, and Congo red, respectively. Adsorption experiments are carried out for aqueous solution of chrysoidine for two different concentrations (400 and 700 mg/L) at three different temperatures (30, 50, and 70 °C) and at a pH of 4.4. It has been observed that the adsorption capacity increases significantly with temperature as shown in Fig. 2.4a for the initial chrysoidine concentration of 400 mg/L. The percentage adsorption increases from about 94 to 99% for the feed dye concentration of 400 mg/L and about 80 to 87% for the feed dye concentration of 700 mg/L, at the end of experiment, when temperature is raised from 30 to 70 °C. This endothermic nature of adsorption is due to the positive ΔH^0 value as shown in Table 2.4a.

In order to observe the effect of temperature on the adsorption capacity, experiments are carried out for 100 mg/L eosin at three different temperatures (30, 40, and 50 °C) using 1.0 g of activated carbon per liter of the solution. It has been observed that with increase in temperature, adsorption capacity decreases as shown in Fig. 2.4b. This is due to the negative value of ΔH^0 value (refer to Table 2.4b).

Experiments are carried out to observe the effect of temperature on the extent of adsorption for Congo red of different initial concentration (50, 100, and 200 mg/L)

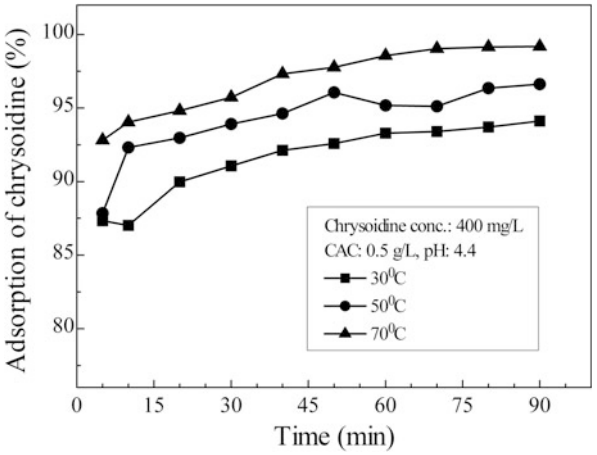

Fig. 2.4a Effect of temperature on adsorption capacity for 400 mg/L of feed chrysoidine (Reproduced from Purkait et al. (2004). With permission from Taylor & Francis Ltd)

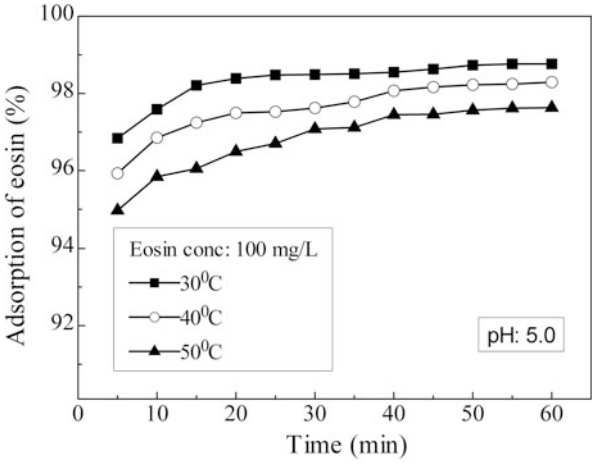

Fig. 2.4b Effect of temperature on adsorption capacity for 100 mg/L of feed eosin (Reproduced from Purkait et al. (2005). With permission from Elsevier)

in aqueous solution at three different temperatures (e.g., 30, 40, and 50 °C) and at neutral pH. It has been observed that the adsorption capacity increases significantly with temperature as shown in Fig. 2.4c for the initial Congo red concentration of 100 mg/L. This is because of positive ΔH^0 value as shown in Table 2.4c.

The thermodynamic parameters ΔG^0, $\Delta S,^0$ and ΔH^0 for the adsorption of chrysoidine, eosin, and Congo red have been determined by using the following equations (Khan et al. 1995):

$$\Delta G^0 = \Delta H^0 - T\Delta S^0 \tag{2.1}$$

$$\log(q_e/C_e) = \frac{\Delta S^0}{2.303R} + \frac{-\Delta H^0}{2.303RT} \tag{2.2}$$

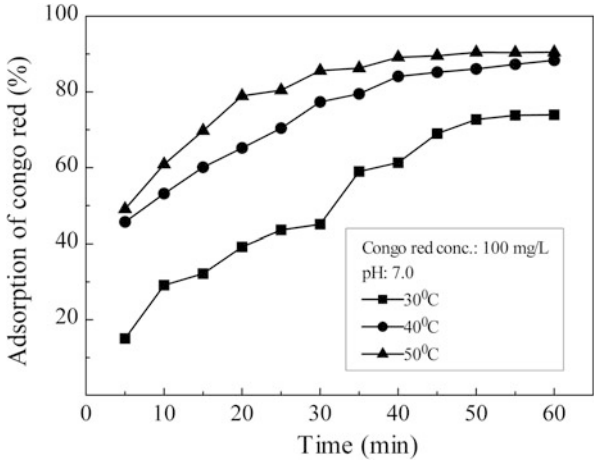

Fig. 2.4c Effect of temperature on adsorption capacity for 100 mg/L of feed Congo red (Reproduced from Purkait et al. (2007). With permission from Elsevier)

where q_e is the amount of dye adsorbed per unit mass of activated carbon (mg/g), C_e is equilibrium concentration (mg/L), and T is temperature in Kelvin. q_e/C_e is called the adsorption affinity. It may be noted here that the experimental data considered here for the calculation of the thermodynamic parameters, namely, ΔG^0,ΔH^0, and ΔS^0, are in the linear range of the equilibrium adsorption isotherm (e.g., for chrysoidine, $q_e$varies from 2.5 to 3.0 mmol/g and $C_e$varies from 0.012 to 0.2 mmol/L as shown in Fig. 2.5a). The values of Gibbs free energy (ΔG^0) have been calculated by knowing the enthalpy of adsorption (ΔH^0) and the entropy of adsorption (ΔS^0). ΔS^0 and ΔH^0 are obtained from a plot of $\log(q_e/C_e)$ versus $\frac{1}{T}$, from Eq. (2.2). Once these two parameters are obtained, ΔG^0 is determined from Eq. (2.1). The values ofΔG^0, ΔH^0, and $\Delta S^0$are listed in Tables 2.2a, 2.2b and 2.2c for chrysoidine, eosin, and Congo red, respectively.

Gibbs free energy (ΔG^0) for all the three dyes is negative (as shown in Tables 2.2a, 2.2b, 2.2c). This indicates that the adsorption process is spontaneous for all the three dyes. Adsorption of chrysoidine and Congo red is endothermic in nature (since ΔH^0 value is positive; refer to Tables 2.2a and 2.2c). On the other hand, eosin adsorption is exothermic in nature (as ΔH^0 value is negative; refer to Table 2.2b). The positive value of ΔS^0 for chrysoidine and Congo red (refer to Tables 2.2a and 2.2c) dictates that the adsorbed dye molecules on the activated carbon surface are organized in a more random fashion compared to those in the aqueous phase. Similar observations have been reported in the literature (Bhattacharyya and Sharma 2003). For eosin, the negative value of ΔS^0 (refer to Table 2.2b) suggests decreased randomness at the solid solution interface during adsorption (Manju et al. 1998).

Table 2.2a Thermodynamic parameters for adsorption of chrysoidine in activated charcoal at different temperature and dye concentrations

Adsorbent (g/L)	Chrysoidine (mg/L)	ΔH^0 (kJ/mol)	ΔS^0 (J/mol.K)	$-\Delta G^0$(kJ/mol) at temperature		
				303 K	323 K	343 K
0.5	400	43.6	171.4	8.3	11.8	15.2
1.0	700	48.9	180.9	5.9	9.6	13.2
Mean		46.3	176.2	7.1	10.7	14.2

Reproduced from Purkait et al. (2004). With permission from Taylor & Francis Ltd

Table 2.2b Thermodynamic parameters for adsorption of eosin in activated charcoal at different temperature and 100 mg/L of eosin

Eosin (mg/L)	ΔH^0 (kJ/mol)	ΔS^0 (J/mol.K)	$-\Delta G^0$ (kJ/mol) at temperature		
			303 K	313 K	323 K
100	27.0	52.6	11.0	10.5	10.0

Reproduced from Purkait et al. (2005). With permission from Elsevier

Table 2.2c Thermodynamic parameters for adsorption of Congo red in activated charcoal at different temperature and dye concentrations

Congo red (mg/L)	ΔH^0 (kJ/mol)	ΔS^0 (J/mol.K)	$-\Delta G^0$(kJ/mol) at temperature		
			303 K	313 K	323 K
50	21.5	86.8	4.8	5.7	6.6
100	51.1	178.1	2.9	4.6	6.4
200	10.1	34.5	0.3	0.67	1.0
Mean	27.6	99.8	2.7	3.7	4.7

2.2.1.1 Langmuir Adsorption Isotherm

Langmuir adsorption isotherm is applicable to explain the equilibrium data for many adsorption processes. The basic assumption of this process is the formation of monolayer of adsorbate on the outer surface of adsorbent, and after that no further adsorption takes place. The expression of the Langmuir model is given as follows (Ozacar and Sengil 2003):

$$q_e = \frac{QbC_e}{1 + bC_e} \tag{2.3}$$

A linear form of this expression is

$$\frac{1}{q_e} = \frac{1}{Q} + \frac{1}{Qb} \cdot \frac{1}{C_e} \tag{2.4}$$

where $q_e$is the amount of adsorbate adsorbed per unit weight of adsorbent (mg/g) and C_e is the equilibrium concentration of adsorbate (mg/L). The constant Q and

b are the Langmuir constants and are the significance of adsorption capacity (mg/g) and energy of adsorption (l/mg), respectively. Values of Q and b are calculated from the intercept and slope of the plot $1/q_e$ versus $1/C_e$.

2.2.1.2 Freundlich Adsorption Isotherm

This model is an indicative of the extent of heterogeneity of the surface of adsorbent and is given as follows:

$$q_e = K_F C_e^{1/n} \tag{2.5}$$

where K_F and n are Freundlich constants. A linear form of the Freundlich expression is as follows:

$$\log q_e = \log K_F + \frac{1}{n}\log C_e \tag{2.6}$$

The constants K_F and n are the Freundlich constants and are the significance of adsorption capacity and intensity of adsorption, respectively. Values of K_F and n are calculated from the intercept and slope of the plot $\log q_e$ versus $\log C_e$.

Adsorption isotherms of chrysoidine, eosin, and Congo red on activated carbon at 30 °C are shown in Figs. 2.5a, 2.5b, and 2.5c, respectively. The coefficients of these two isotherm models for the three dyes are given in Table 2.3. These data provide information on the amount of activated carbon required to adsorb a particular mass of dye under specified system conditions. Correlation coefficients are evaluated by fitting the experimental adsorption equilibrium data for three dyes separately using both Langmuir and Freundlich adsorption isotherms and are also shown in Table 2.3. It is found from the correlation coefficients (r^2) that adsorption

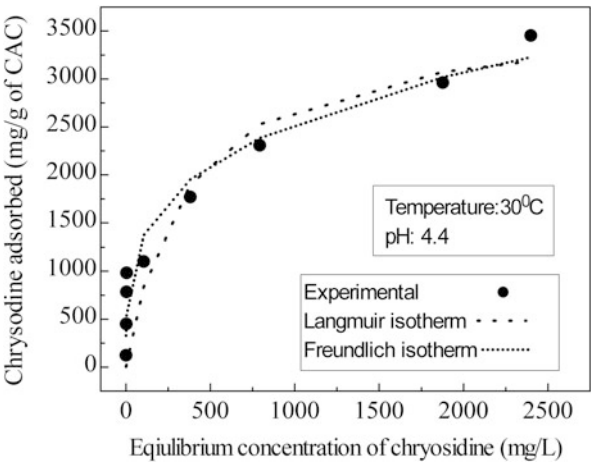

Fig. 2.5a Adsorption isotherms of chrysoidine on activated carbon (Reproduced from Purkait et al. (2004). With permission from Taylor & Francis Ltd)

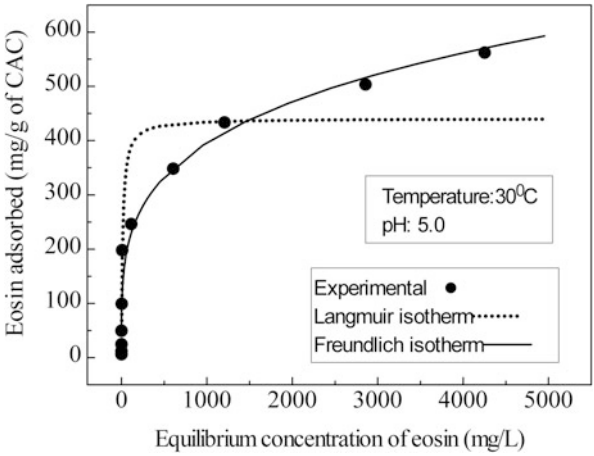

Fig. 2.5b Adsorption isotherms of eosin on activated carbon

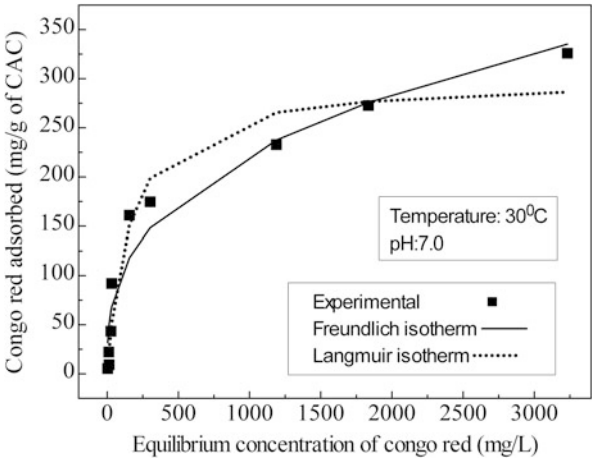

Fig. 2.5c Adsorption isotherms of Congo red on activated carbon (Reproduced from Purkait et al. (2007). With permission from Elsevier)

Table 2.3 Langmuir and Freundlich isotherm constants for adsorption of dyes on activated charcoal

	Langmuir isotherm constant			Freundlich isotherm constant		
Dye	Q (mg/g)	b (l/mg)	r^2	K_F (mg/g(L/mg)$^{1/n}$)	n	r^2
Chrysoidine	3652.0	2.84×10^{-3}	0.94	384.2	3.66	0.97
Eosin	571.4	4.35×10^{-3}	0.96	75.5	4.14	0.99
Congo red	300.0	6.50×10^{-3}	0.94	20.78	2.90	0.96

isotherm for the present three dye-activated charcoal systems is best explained by Freundlich equation.

2.2.1.3 Adsorption Kinetics

The kinetics of adsorption of chrysoidine, eosin, and Congo red on activated carbon have been described using both first- and pseudo-second-order model. The Lagergren's equation for first-order kinetics is as follows:

$$\log(q_e - q_t) = \log q_e - \frac{k_1 t}{2.303} \tag{2.7}$$

The expression for pseudo-second-order rate equation is given as (Ho et al. 1996)

$$\frac{t}{q_t} = \frac{1}{k_2 q_e^2} + \frac{t}{q_e} \tag{2.8}$$

where q_e and q_t are the amounts of dye adsorbed (mg/g) at equilibrium and at any time t and k_1 is the rate constant (min^{-1}). Figures 2.6a, 2.6b, and 2.6c show (t/q_t) versus t plot for pseudo-second-order kinetics for chrysoidine, eosin, and Congo red, respectively. In Eq. (2.8), k_2 (g/mg min) is the rate constant for the pseudo-second-order adsorption kinetics. The slope of the plot (t/q_t) versus t gives the value of q_e, and from the intercept, k_2 can be calculated. The values of k_1, k_2, and correlation coefficients (r^2), both in the first and pseudo-second-order kinetics, are presented in Tables 2.4a, 2.4b, and 2.4c for chrysoidine, eosin, and Congo red, respectively. It may be observed from Tables 2.4a, 2.4b, and 2.4c that the adsorption of chrysoidine, eosin, and Congo red on activated carbon follows pseudo-second-order kinetics more closely.

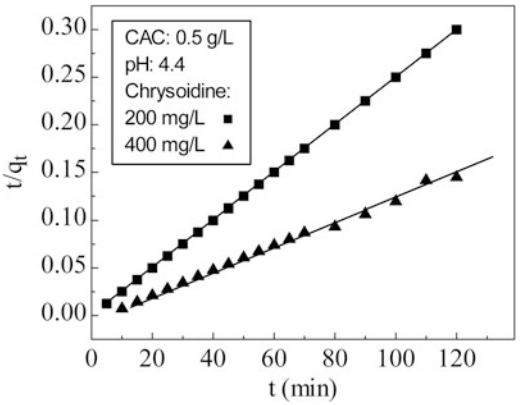

Fig. 2.6a Plot of the pseudo-second-order kinetic model for adsorption of chrysoidine on activated carbon (0.5 g/L). Feed chrysoidine: 200 and 400 mg/L (Reproduced from Purkait et al. (2004). With permission from Taylor & Francis Ltd)

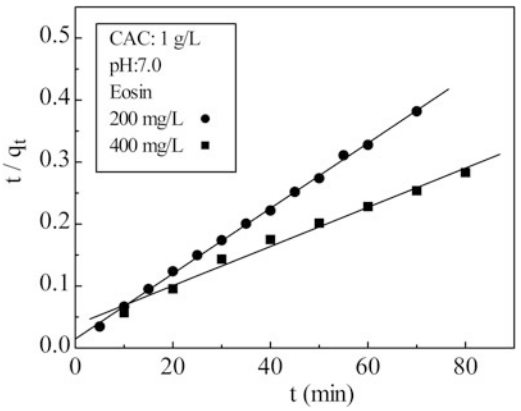

Fig. 2.6b Plot of the pseudo-second-order kinetic model for adsorption of eosin on activated carbon (1.0 g/L). Feed eosin: 200 and 400 mg/L (Reproduced from Purkait et al. (2005). With permission from Elsevier)

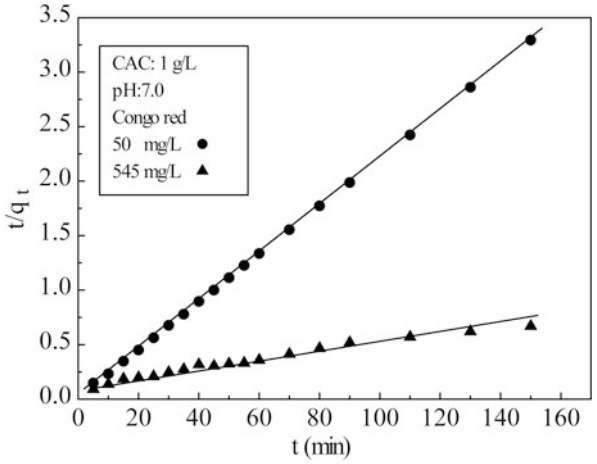

Fig. 2.6c Plot of the pseudo-second-order kinetic model for adsorption of Congo red on activated carbon (1.0 g/L). Feed Congo red: 50 and 545 mg/L

Table 2.4a Comparison of the first- and second-order adsorption rate constants, calculated and experimental q_e value for chrysoidine on activated charcoal

Chrysoidine (c_0) (mg/L)	q_e, exp t (mg/g)	First-order			Pseudo-second-order		
		q_e, *fit* (mg/g)	k_1 (1/min)	r^2	q_e, *fit* (mg/g)	k_2 (g/mg min)	r^2
Feed CAC: 0.25 g/L							
200	737.2	710.4	0.30	0.422	751.8	5.4×10^{-4}	0.998
250	831.9	770.2	0.46	0.202	833.3	3.5×10^{-4}	0.997
300	907.5	890.6	0.71	0.210	917.4	13.5×10^{-4}	0.999
400	972.0	921.9	0.44	0.395	980.4	4.3×10^{-4}	0.998
Feed CAC: 0.50 g/L							
200	400.0	399.4	1.08	0.454	400.0	7.4×10^{-1}	0.998
250	500.0	495.6	0.62	0.576	500.0	5.4×10^{-3}	0.999
300	599.5	589.9	0.55	0.547	602.4	2.3×10^{-3}	0.999
400	759.6	738.2	0.56	0.255	787.4	4.9×10^{-4}	0.998

Reproduced from Purkait et al. (2004). With permission from Taylor & Francis Ltd

Table 2.4b Comparison of the first- and second-order adsorption rate constants, calculated and experimental q_e value for eosin on activated charcoal

Eosin (c_0) (mg/L)	$q_{e,exp}$ (mg/g)	First-order			Pseudo-second-order		
		$q_{e,fit}$ (mg/g)	k_1 (1/min)	r^2	$q_{e,fit}$ (mg/g)	k_2 (g/mg min)	r^2
Feed CAC: 1.0 g/L							
200	175.0	152.3	6.7×10^{-2}	0.91	173.4	5.4×10^{-4}	0.998
400	286.0	232.2	4.4×10^{-2}	0.86	302.1	4.3×10^{-4}	0.998

Reproduced from Purkait et al. (2005). With permission from Elsevier

Table 2.4c Comparison of the first- and second-order adsorption rate constants, calculated and experimental q_e value for Congo red on activated charcoal

Congo red (c_0) (mg/L)	$q_{e,exp}$ (mg/g)	First-order			Pseudo-second-order		
		$q_{e,fit}$ (mg/g)	k_1 (1/min)	r^2	$q_{e,fit}$ (mg/g)	k_2 (g/mg min)	r^2
Feed CAC: 1.0 g/L							
50	45.7	2.2	1.8×10^{-2}	0.925	45.9	2×10^{-2}	0.999
100	76.2	75.0	4.1×10^{-2}	0.879	88.5	5.3×10^{-2}	0.987
380	171.1	119.0	2.9×10^{-2}	0.964	181.8	4.5×10^{-2}	0.997
545	183.1	144.8	3.0×10^{-2}	0.978	207.5	2.5×10^{-2}	0.995

Reproduced from Purkait et al. (2007). With permission from Elsevier

2.2.2 Column Adsorption

Column adsorptions studies are essential for design of industrial scale fixed-bed adsorber system. Figure 2.7 shows the breakthrough curves for different bed depths. It may be observed from Fig. 2.8 that the breakthrough time (duration for zero column outlet concentration) increases from 18 to 39 h, when the bed depth is increased from 4.5×10^{-2} m to 7.0×10^{-2} m, for the same flow rate of 0.18 L/hr. The shape and the gradient of the breakthrough curves for the two bed depths are almost identical.

2.3 Generalized Shrinking Core Model for Batch Adsorption Data

To develop a mathematical model that describes the adsorption dynamics, the following information are generally required:

1. A complete description of equilibrium behavior, i.e., the maximum level of adsorption attained in a sorbent/sorbate system as a function of the sorbate liquid-phase concentration

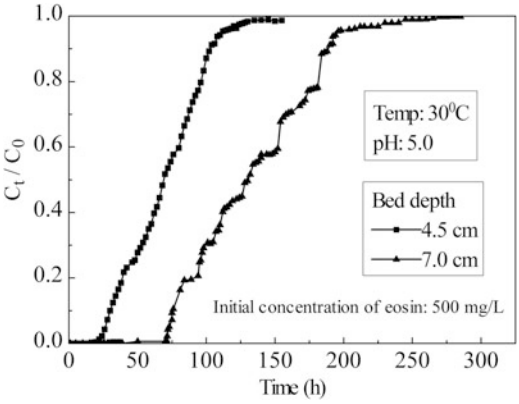

Fig. 2.7 Variation of the breakthrough curve with bed depth (Reproduced from Purkait et al. (2005). With permission from Elsevier)

2. Mathematical representation of associated rate of adsorption, which is controlled by the resistances within the sorbent particles

In adsorption, mainly two resistances prevail – the external liquid film resistance and the resistance in the adsorbent particle. The intraparticle diffusion resistance may be neglected for solutes that exhibit strong solid to liquid-phase equilibrium solute distribution, in the initial period of operation. However, even for such systems, the above assumption leads to errors that are substantial beyond the first few minutes if the agitation is high (Mathews and Weber 1976). So, both the resistances are important for kinetic study (Chatzopoulos et al. 1993; McKay 1984; Costa et al. 1987; Komiyama and Smith 1974; Liapis and Rippin 1977).

The external liquid film resistance is characterized by the external liquid film mass transfer coefficient (k_f). The mass transport within the adsorbent particles is assumed to be a pore diffusion (Dedrick and Beckman 1967; Weber and Rumer 1965; Furusawa and Smith 1973; McKay 1982) or homogeneous solid diffusion process (McKay 1982; Hand et al. 1983; Kapoor et al. 1989).

The pore diffusion model outlined in this paper is based on the unreacted shrinking core model (Yen 1968; Levenspiel 1972) with pseudo-steady-state approximation. This model has mostly been applied to gas-solid non-catalytic reactions, but a number of liquid-solid reactions also have been analyzed using this model (Neretnieks 1976; Spahn and Schlunder 1975). In the pore diffusion model, there is adsorption of the adsorbate into the pores with a cocurrent solute distributed all along the pore wall.

The assumptions made in this model are as follows:

(a) Pore diffusivity is independent of concentration.
(b) Adsorption isotherm is irreversible.
(c) Pseudo-steady-state approximation is valid.
(d) The driving force in both film and particle mass transfer is directly proportional.
(e) Adsorbent particles are spherical.

The major limitation of this model is that it is specific to the nature of isotherm. This means that the model available in literature is most suitable for Langmuir-type

isotherm, i.e., formation of a monolayer of adsorbate on the adsorbent. Besides, this model is only applicable for higher initial adsorbate concentration in solution so that the batch process operating line intercepts the invariant zone of isotherm. For example, for Astrazone blue-silica system, the literature model is applicable for $C_0 >> 200$ mg/lit (McKay 1984). The present model, which is more generalized, overcomes the above limitations. The model proposed, here in, can be applied to wide ranges of initial adsorbate concentrations for all possible nature of isotherms. The system reported here is adsorption of Astrazone blue dye on Sorbsil Silica.

The equations considered for the kinetics of the adsorption process for spherical adsorbent particles for the present model are as follows:

The mass transfer from external liquid phase can be written as

$$N(t) = 4\pi R^2 K_f (C_t - C_{et}) \tag{2.9}$$

The diffusion of solute through the pores as per Fick's law can be written as

$$N(t) = \frac{4\pi D_p C_{et}}{\left[\frac{1}{R_f} - \frac{1}{R}\right]} \tag{2.10}$$

where D_p is the effective diffusivity in the porous adsorbent (Fogler 1997).

The mass balance on a spherical element of adsorbate particle can be written as

$$N(t) = -4\pi {R_f}^2 Y_{et} \rho \left[\frac{dR_f}{dt}\right] \tag{2.11}$$

The average concentration on adsorbent particle can be written as

$$\overline{Y_t} = Y_{et}\left[1 - \left(\frac{R_f}{R}\right)^3\right] \tag{2.12}$$

The differential mass balance over the system by equating the decrease in adsorbate concentration in the solution with the accumulation of the adsorbate in the adsorbent can be written as

$$N(t) = -V\left(\frac{dC_t}{dt}\right) = W\left(\frac{d\overline{Y_t}}{dt}\right) \tag{2.13}$$

The dimensionless terms used for simplification are as follows:

$$C_t^* = \frac{C_t}{C_0}, r = \frac{R_f}{R}, Bi = \frac{k_f R}{D_p}, \quad Ch = \frac{W}{VC_0}, {C_{et}}^* = \frac{C_{et}}{C_0} \text{ and } \tau = \frac{D_p t}{R^2}$$

Simplifying Eqs. (2.9) and (2.10)

$$C_{et}{}^{*} = \frac{Bi(1-r)C_t^*}{[r+Bi(1-r)]} = g_1\left(C_t^*, r\right) \tag{2.14}$$

Now differentiating the above equation with respect to τ

$$\frac{dC_{et}^*}{d\tau} = \frac{Bi(1-r)}{r+Bi(1-r)}\frac{dC_t^*}{d\tau} - \frac{BiC_t^*}{[r+Bi(1-r)]^2}\frac{dr}{d\tau} \tag{2.15}$$

From the equilibrium relationship

$$Y_e(t) = g_2\left(C_{et}^*\right) \tag{2.16}$$

where g_2 is any equilibrium isotherm relationship. Simplifying Eqs. (2.9) and (2.11)

$$\left(\frac{dr}{d\tau}\right) = \frac{-Bi\left(\frac{C_0}{\rho Y_e}\right)\left(C_t^* - C_{et}{}^{*}\right)}{r^2} \tag{2.17}$$

Simplifying Eqs. (2.12) and (2.13)

$$\left(\frac{dC_t^*}{d\tau}\right) + Ch\left(1-r^3\right)\left(\frac{dY_{et}}{d\tau}\right) = 3Ch \cdot Y_{et}r^2\left(\frac{dr}{d\tau}\right) \tag{2.18}$$

For Langmuir isotherm

$$Y_{et} = \frac{Y_sC_{et}}{1+k_0C_{et}} = \frac{Y_sC_0C_{et}^*}{1+k_0C_0C_{et}^*} = \frac{Y_{es}C_{et}^*}{1+k_0^*C_{et}^*} \tag{2.19}$$

where $Y_{es} = Y_sC_0$ and $k_0{}^{*} = k_0C_0$.

The time derivative of Eq. (2.19) becomes

$$\frac{dY_{et}}{d\tau} = \frac{Y_{es}}{\left(1+k_0^*C_{et}^*\right)^2}\frac{dC_{et}^*}{d\tau} \tag{2.20}$$

Combining Eqs. (2.14), (2.18), and (2.20) and after algebraic manipulation, the following expression is obtained (for Langmuir-type isotherm):

$$\left(\frac{dC_t^*}{d\tau}\right) = \left(N/M\right)\left(\frac{dr}{d\tau}\right) \tag{2.21}$$

where $M = 1 + Ch\left(1-r^3\right)\dfrac{Y_{es}Bi(1-r)}{\left(1+k_0^*C_{et}^*\right)^2[r+(1-r)Bi]}$ and,

$N = 3ChY_{et}r^2 + \dfrac{ChY_{es}Bi(1-r^3)C_t^*}{\left(1+k_0^*C_{et}^*\right)^2[r+(1-r)Bi]^2}$. Using Eq. (2.14), Eq. (2.17) may be written as

$$\frac{dr}{d\tau} = \frac{-Bi\left(\frac{C_0}{\rho Y_e}\right)\left(C_t^* - C_{et}{}^*\right)}{r^2} = f_1\left(C_t^*, r\right) \tag{2.22}$$

Using Eqs. (2.14) and (2.22), Eq. (2.21) may be expressed as

$$\left(\frac{dC_t^*}{d\tau}\right) = \frac{N\left(C_t^*, r\right) f_1\left(C_t^*, r\right)}{M\left(C_t^*, r\right)} = f_2\left(C_t^*, r\right) \tag{2.23}$$

The initial conditions for Eqs. (2.22) and (2.23), $C_0 = 1.0$ and $r = 1.0$ at time, $\tau = 0.0$. Equations (2.22) and (2.23) can be solved to find the bulk concentration at any time "t" if we know all the process parameters. The two process parameters – the external mass transfer coefficient (k_f) and internal effective diffusivity (D_p) – are unknown to us. These two parameters are estimated by optimizing the experimental concentration profile as outlined in the next section.

2.3.1 Numerical Analysis

The above set of equations are numerically solved using fourth-order Runge-Kutta of step size (dτ) of the order 10^{-5} along with a nonlinear optimization technique (Levenberg-Marquardt) to estimate the two process parameters described above, so that the experiment kinetic profile (i.e., bulk concentration versus time) is matched. For this purpose, optimization subroutine UNLSF/DUNLSF from IMSL math library has been used.

The adsorption systems studied here encompass Radke-Prausnitz isotherm (Tables 2.5 and 2.6). The systems considered here are (1) Astrazone blue dye on silica, (2) para-nitrophenol on granular activated carbon from Lurgi, and (3) toluene on F300 activated carbon. The experimental data on kinetics and the isotherm constants have been reported in literature (McKay 1984; Costa et al. 1987; Chatzopoulos et al. 1993).

The adsorption of Astrazone blue on silica follows Langmuir isotherm (McKay 1984). The isotherm constants are $Y_s = 0.5$ lit/g and $K_0 = 0.016$ lit/mg, where Y_e in mg/g and C_e in mg/l. For $W = 17$ g, $V = 1.7$ l, $R = 0.3025$ mm, and $\rho = 2.2$ g/cc, the concentration decay data for $C_0 = 520$ mg/l has been used to determine the unknown process parameters using the above numerical procedure as shown in Fig. 2.8a. The estimated values of the parameters are as follows: $k_f = 130.0 \times 10^{-6}$ cm/s and $D_p = 16.16 \times 10^{-9}$ cm^2/s. These values of k_f and D_p are used to simulate the adsorption kinetics for different operating conditions. It is interesting to note that the estimated values of k_f and D_p are close to the values reported by Mckay (1984), i.e., $k_f = 80 \times 10^{-6}$ cm/s and $D_p = 18 \times 10^{-9}$ cm^2/s. The experimental observations and the model-simulated concentration profiles for different initial dye

Table 2.5 Radke-Prausnitz isotherm constants $\left[\left(\frac{1}{Y_e}\right) = \left(\frac{1}{AC_e}\right) + \left(\frac{1}{BC_e^{\delta}}\right)\right]$

Isotherm	T (°C)	A (L/g)	B (L/g)	δ
Radke-Prausnitz	10	958.91	2.523	0.195
	25	608.16	2.269	0.188
	40	315.37	2.078	0.196

Table 2.6 Model parameters using Radke-Prausnitz isotherm at various temperatures

Temp. (°C)	$k_f \times 10^5$ (m/s)	$D_p \times 10^8$ (m^2/s)
10	11.48	
25	19.10	6.0
40	27.86	

concentrations, masses of silica, and particle sizes of silica have been shown in Figs. 2.8b, 2.8c and 2.8d, respectively. From the above figures, it may be observed that beyond 120 min (2 h) of the process, the model underpredicts the bulk concentration profile. This may be due to the increase of the resistance inside the micropores which inhibits the process of adsorption. The present model can be used for multicomponent adsorption processes and also with concentration-dependent diffusivity. The model is useful to estimate k_f and D_p values, which are required for the design of fixed-bed adsorber.

2.4 Discussion of Mathematical Model Analysis

The adsorption experiments in the fixed-bed column are carried out to study the adsorption dynamics and quantify the breakthrough curve. One of the crucial aspects of design of adsorption columns for any separation process is the prediction of the breakthrough time. This is necessary to estimate the lifetime of the adsorption bed and its process efficiency. There have been several mathematical models developed in the past based on different assumption justifying the simplicity in the calculations.

2.4.1 Thomas Model (Thomas 1944)

Thomas solution is the most general and widely used equation for modeling performance of fixed-bed adsorption. The Thomas model assumes second-order reversible Langmuir kinetics of the adsorption-desorption process. Ideally the model is suitable for situations where the external and internal diffusion resistances are small. This is particularly true for adsorption scenarios in most liquid systems and therefore is most relevant for adsorption in aqueous environment. The expression describing the output concentration C_t/C_0 is given by

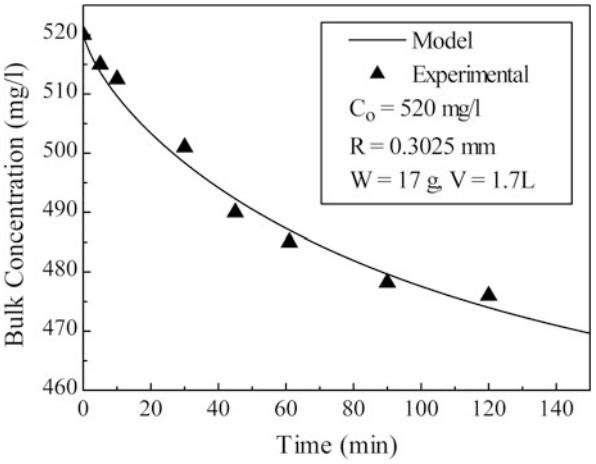

Fig. 2.8a Adsorption of Astrazone blue dye on silica

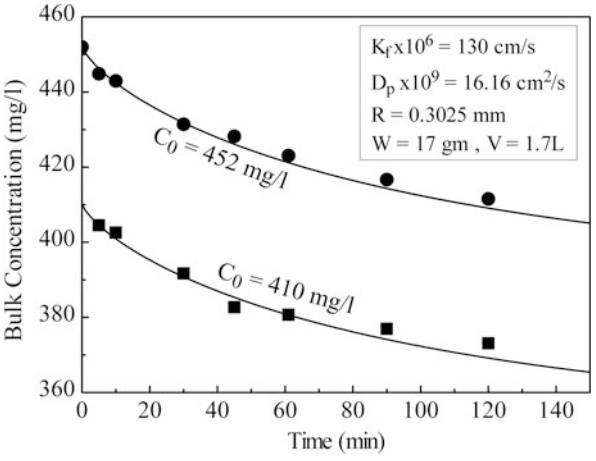

Fig. 2.8b Effect of initial adsorbate concentration. *Solid lines* are the model predictions and *symbols* are the experimental data

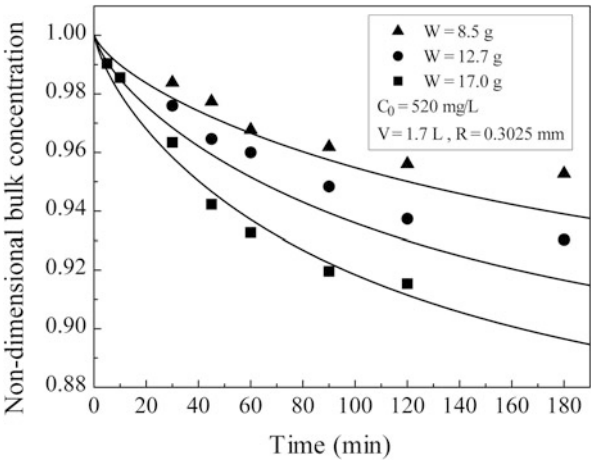

Fig. 2.8c Effect of the mass of adsorbent on concentration decay. *Solid lines* are the model predictions and *symbols* are the experimental data

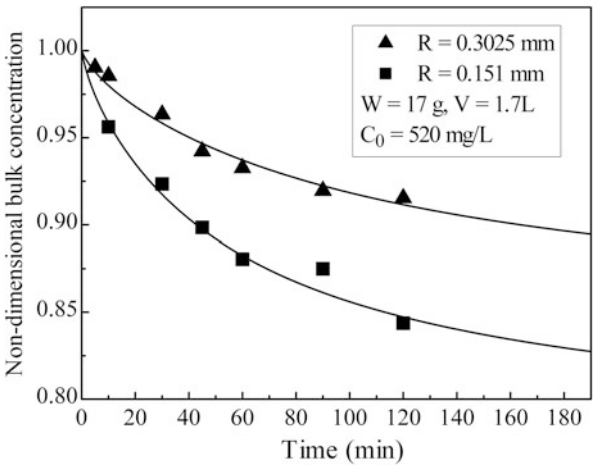

Fig. 2.8d Effect of silica particle size on concentration decay. *Solid lines* are the model predictions and *symbols* are the experimental data

$$\frac{c_t}{c_0} = \frac{1}{1 + \exp\left(k_{Th} q_e{}^{Z/Q - k_{Th} c_0 t}\right)} \tag{2.24}$$

where k_{Th} is the model parameter obtained from nonlinear regression of the output concentration with time. The parameter q_e is the maximum adsorption capacity of the adsorbent.

2.4.2 Adams-Bohart Model (Bohart and Adams 1920)

The Adams-Bohart model considers that the adsorption rate is proportional to both the adsorbent leftover capacity and the concentration of the adsorbate species in the solution. The Adams-Bohart model is originally applied for prediction of adsorption behavior in gas-solid systems, but later on extended to liquid streams. It assumes that the adsorption rate is proportional to the residual capacity of the adsorbent and adsorbate concentration. Since the external mass transfer is not taken into account, it is particularly not suitable for describing the system at high flow rate and concentration. Theoretically, the model is applicable for predictions at early times, when $C/C_0 << 1$. The mathematical equation describing the output concentration is represented by Eq. (2.25):

$$\frac{c_t}{c_0} = \exp\left(k_{AB} c_0 t - k_{AB} q_e \frac{Z}{Q}\right) \tag{2.25}$$

where k_{AB} is the model parameter obtained from nonlinear regression of the experimental data.

2.4.3 Yoon-Nelson Model (Yoon and Nelson 1984)

The Yoon-Nelson model is based on the assumption that the probability of adsorption for each molecule decreases proportionately on the probabilities of the adsorbate adsorption and breakthrough. One of the features of the model is that the product of the parameters $K_{\mathrm{yn}}\tau_{\mathrm{yn}}$is constant for a particular adsorbent-adsorbate combination and independent on the operating conditions. This is a fairly simple model which does not require any knowledge of the adsorption capacity or type of the adsorbent:

$$\frac{c_t}{c_0 - c_{\mathrm{t}}} = \exp(k_{\mathrm{YN}}t - \tau k_{\mathrm{YN}}) \tag{2.26}$$

where τ and k_{YN} are the model parameters obtained from nonlinear regression of the experimental data.

2.4.4 Clark Model (Clark 1987)

This model is based on the application of the mass transfer concept in combination with Freundlich equilibrium isotherm. The adsorption equilibrium isotherm satisfying Freundlich relationship can only be used for predicting the breakthrough profile of the adsorption column. The semiempirical relationship is presented in Eq. (2.27):

$$\frac{c_{\mathrm{t}}}{c_0} = \left(\frac{1}{1 + A\exp(-rt)}\right)^{1/(n-1)} \tag{2.27}$$

where A and r are the model constants obtained from nonlinear regression analysis. The constant 1/n is obtained from the Freundlich isotherm equation.

2.4.5 Bed Depth/Service Time (BDST) Model (Goel et al. 2005)

The BDST model is the linearized form of the Adams-Bohart model. The main consideration here is the assumption that the intraparticle diffusion and external mass transfer resistance is negligible and the adsorption kinetics is controlled by the surface chemical reaction between the adsorbate and adsorbent, which is generally uncommon in real systems. The popularity of the BDST is due to its simplicity in predicting breakthrough behavior owing to its rapid analysis. The expression predicting the breakthrough profile (C_{t}/C_0) is given by

$$\frac{c_0}{c_t} = 1 + K_{BDST}\exp\left(\frac{q_e Z}{Q} - c_0 t\right) \tag{2.28}$$

where K_{BDST} is the model parameter determined by the nonlinear regression analysis of the experimental data. Although the BDST model provides a simple and comprehensive approach for evaluating sorption column test, its validity is limited and does not involve any sound understanding of the implicit transport mechanism (Bohart and Adams 1920; Poots et al. 1976a; Faust and Aly 1987). One of the major limitations of this model is the symmetry of the logistic function (S-shaped curve) around its midpoint $t = N_0 Z/C_0 U_0$ and $C = C_0/2$, which is not true for most breakthrough profiles. Therefore, a more detailed adsorption bed modeling based on the physical transport laws of pore diffusion is necessary for accuracy of the model prediction and scaling up of the process.

2.4.6 Pore Diffusion-Adsorption Model

The 1D single species convective-diffusive equation (Kunii and Levenspiel 1991) is described by Eq. (2.29):

$$\frac{\partial C}{\partial t} = D_L \frac{\partial^2 C}{\partial z^2} - v\frac{\partial C}{\partial z} - \left(\frac{3k_f}{a_p}\right)\left(\frac{1-\varepsilon}{\varepsilon}\right)\rho_s(C - C_e) \tag{2.29}$$

where the generation term accounted is dependent on the solid-fluid mass transfer rate and is linearly proportional to the concentration difference and C_e is the adsorbate concentration at the adsorbent-bulk interface. The solution of Eq. (2.29) provides information of the transient solute concentration at various bed depths. In deriving Eq. (2.29), by the material balance analysis, it is inherently assumed that all the interparticle void space in the bed is saturated and the fluid velocity is uniform and unhindered throughout. The initial and boundary conditions of Eq. (2.29) are

$$\text{at t} = 0, C = C_0 \quad \text{for } z = 0 \text{ and } C = 0 \text{ for} \quad 0 < z \le L \tag{2.30a}$$

$$\text{at } z = 0, \quad D_L \frac{\partial C}{\partial z} + V(C_0 - C) = 0 \tag{2.30b}$$

$$\text{and at } z = \text{L}, \quad \frac{\partial C}{\partial z} = 0 \tag{2.30c}$$

The intra-pellet adsorption is described by the pore diffusion transport model. Intraparticle mass transport is characterized by the pore diffusion coefficient D_p. The mass balance equation for the liquid phase (pore) in a spherical particle can be written as

$$\varepsilon_p \frac{\partial C_p}{\partial t} + (1-\varepsilon_p)\rho_s \frac{\partial q}{\partial t} = D_p \left(\frac{\partial^2 C_p}{\partial r^2} + \frac{2}{r}\frac{\partial C_p}{\partial r} \right) \tag{2.31}$$

where C_p is the contaminant concentration inside the particle and $\varepsilon_p$is particle porosity. Assuming instantaneous equilibrium $\frac{\partial q}{\partial t} = \frac{\partial C_p}{\partial t}\frac{\partial q}{\partial C_p}$. Modifying Eq. (2.31), we get (Singha et al. 2012),

$$\frac{\partial C_p}{\partial t} = \frac{1}{\left[1 + (1-\varepsilon_p)\rho_s \frac{\partial q}{\partial C_p}\right]} \left(\frac{D_p}{\varepsilon_p}\right) \left(\frac{\partial^2 C_p}{\partial r^2} + \frac{2}{r}\frac{\partial C_p}{\partial r} \right) \tag{2.32}$$

The initial condition ($t = 0$) is given by $C_p = 0$ for $0 < r < a_p$.

The symmetry condition at the particle center ($r = 0$) and continuity of the concentration on the external surface of the adsorbent bed are simultaneously expressed as

$$\text{at } r = 0, \frac{\partial C_p}{\partial r} = 0 \tag{2.33a}$$

$$\text{and at } r = a_p, k_f(C_p - C_e) = D_p \varepsilon_p \frac{\partial C_p}{\partial r} \tag{2.33b}$$

2.5 Various Types of Adsorbents Used for Dye Adsorption

A summary of the various low-cost adsorbents for dye removal as studied by several researchers in the past is presented in Tables 2.7, 2.8 and 2.9. Natural materials or the wastes/by-products of industries or synthetically prepared materials, which cost less and can be used as such or after some minor treatment as adsorbents, are generally called low-cost adsorbents. Generally, the low-cost adsorbents are usually branded as substitutes for activated carbons because of their similar wide usage; however, in a clear sense, they are essentially substitutes for all available expensive adsorbents. These alternative low-cost adsorbents (Gupta et al. 2009) may be categorized in two ways (1) based on their availability, for, e.g., natural materials such as coal, wood, lignite, peat, etc., or agricultural/industrial/domestic wastes; or by-products such as sludge, slag, red mud, fly ash, etc., or synthesized products; and (2) depending on their nature, for, e.g., organic or inorganic. The adsorbents listed in Table 2.7, 2.8, and 2.9 provide useful information about the type and capacity of alternative adsorbents without going into too much detail of the preparation process.

Table 2.7 Adsorption capacities of commercial activated carbon and other alternative adsorbents for removal of acid dyes

Adsorbent	Adsorbate	Surface area (m^2/g)	Adsorption capacity (mg/g)	Concentration range (mg/L)	Source
GAC Filtrasorb 400	Acid blue 40	1100	57.5 mg/g	25–200	Ozacar and Sengil (2002)
Filtrasorb F 400	Acid blue 80	1200	112.3 mg/g	–	Choy et al. (2000)
Filtrasorb F 400	Acid red 114	1200	103.5 mg/g	–	Choy et al. (2000)
Filtrasorb F 400	Acid red 88	–	109 mg/g	–	Venkata Mohan et al. (1999)
Filtrasorb F 400	Acid yellow 117	1200	155.8 mg/g	–	Choy et al. (2000)
GAC Filtrasorb 400	Acid yellow 17	1100	133.3	25–200	Ozacar and Sengil (2002)
PAC	Acid brown 283	1026	22	30–250	Martin et al. (2003)
AC-charcoal	Acid blue	–	100.9	10–25	Choy et al. (1999)
	Acid yellow		128.8		
	Acid red 114		101		
AC rice husk	Acid blue	352	50	1–50	Mohamed (2004)
Blast furnace sludge	Acid blue 113	28	2.1	–	Jain et al. (2003c)
Bentonite	Acid blue 193	767	740.5	–	Ozcan et al. (2004)
Wood sawdust (raw)	Acid blue 25	–	5.92	–	Ho and McKay (1998a)
Treated cotton	Acid blue 25	–	589	–	Bouzaida and Rammah (2002)
Chitosan	Acid blue 25	–	77.4	–	Martel et al. (2001)
Hazelnut shell	Acid blue 25	–	60.2	50–500	Ferrero (2007)
Sawdust-walnut	Acid blue 25	–	37	50–500	Ferrero (2007)
Sawdust-cherry	Acid blue 25	–	32	50–500	Ferrero (2007)

(continued)

Table 2.7 (continued)

Adsorbent	Adsorbate	Surface area (m^2/g)	Adsorption capacity (mg/g)	Concentration range (mg/L)	Source
Sawdust-oak	Acid blue 25	–	27.8	50–500	Ferrero (2007)
Sawdust-pitch pine	Acid blue 25	–	26.2	50–500	Ferrero (2007)
AC-corncob	Acid blue 25	943	1060	–	Juang et al. (2002)
AC-bagasse	Acid blue 25	607	674	–	Juang et al. (2002)
AC-plum kernel	Acid blue 25	1162	904	–	Juang et al. (2002)
Cane pith	Acid blue 25	606.8	673.6	–	Juang et al. (2001)
Bagasse pith	Acid blue 25	–	17.5	10–1000	Chen et al. (2001)
Wood	Acid blue 25	3.8–6.4	7–11.6	–	Poots et al. (1976b)
Maize cob	Acid blue 25	–	41.4	0.05	El-Geundi and Aly (1992)
	Acid red 114		47.7		
Pine sawdust	Acid blue 256	–	280.3	–	Ozacar and Sengil (2005)
AC-pinewood	Acid blue 264	902	1176	–	Tseng et al. (2003)
Dead fungus *Aspergillus niger*	Acid blue 29	–	1.44–13.8	50	Fu and Viraraghavan (2001)
Living biomass *Aspergillus niger*	Acid blue 29	–	6.63	50	Fu and Viraraghavan (2001)
Modified fungal biomass – *Aspergillus niger*	Acid blue 29	–	17.6	46	Fu and Viraraghavan (2002b)
Calcined alunite	Acid blue 40	42.8	212.8	25–200	Ozacar and Sengil (2002)
Activated sewage sludge	Acid blue 74	390	60.0	100–1000	Otero et al. (2003b)
Pyrolyzed sewage sludge	Acid blue 74	80	30.8	100–1000	Otero et al. (2003b)
AC-bagasse	Acid blue 80	1433	391	20–1050	Valix et al. (2004)

(continued)

Table 2.7 (continued)

Adsorbent	Adsorbate	Surface area (m^2/g)	Adsorption capacity (mg/g)	Concentration range (mg/L)	Source
Activated clay	Acid blue 9	–	57.8	–	Ho et al. (2001)
Soy meal hull	Acid blue 92	0.76	114.9	50–150	Arami et al. (2006)
Banana pith	Acid brilliant blue	–	4.4	–	Namasivayam et al. (1998)
Coir pith	Acid brilliant blue	–	16.7	–	Namasivayam et al. (2001)
Leather industry waste	Acid brown	–	2.84–6.24	50–125	Sekaran et al. (1995)
Chitosan	Acid green 25	–	645.1	–	Wong et al. (2004)
	Acid orange 10		922.9		
Banana peel	Acid orange 52	20.6–23.5	21	10–120	Annadurai et al. (2002)
Orange peel	Acid orange 52	20.6–23.5	20.5	10–120	Annadurai et al. (2002)
Sewage sludge	Acid red 1	–	35–73	10–1000	Seredych and Bandosz (2007)
Bagasse pith (raw)	Acid red 114	–	20	10–1000	Chen et al. (2001)
AC from gingelly seed shell	Acid red 114	229.6	102	–	Thinakaran et al. (2008)
AC from cotton-seed shell	Acid red 114	124.3	153.8	–	Thinakaran et al. (2008)
AC from pongam seed shell	Acid red 114	324.8	204.1	–	Thinakaran et al. (2008)
Soy meal hull	Acid red 14	0.76	109.9	50–150	Arami et al. (2006)
Hen feathers	Acid red 51	–	129.1	8.79–52.7	Gupta et al. (2006)
Charfines (raw)	Acid red 88	–	33.3	–	Venkata Mohan et al. (1999)
Lignite coal (raw)	Acid red 88	–	30.9	–	Venkata Mohan et al. (1999)
Bituminous coal	Acid red 88	–	26.1	–	Venkata Mohan et al. (1999)

(continued)

Table 2.7 (continued)

Adsorbent	Adsorbate	Surface area (m^2/g)	Adsorption capacity (mg/g)	Concentration range (mg/L)	Source
Coir pith (raw)	Acid violet	–	1.65	–	Namasivayam et al. (2001)
Orange peel (raw)	Acid violet 17	19.9	–	–	Sivaraj et al. (2001)
Pine sawdust (raw)	Acid yellow 132	–	398.8	–	Ozacar and Sengil (2005)
Calcined alunite	Acid yellow 17	42.8	151.5	25–200	Ozacar and Sengil (2005)
Sawdust carbon	Acid yellow 36	516.3	183.8	–	Malik (2003)
Rice husk carbon	Acid yellow 36	272.5	86.9	–	Malik (2003)
Blast furnace sludge	Acid yellow 36	28	1.4	–	Jain et al. (2003c)
Treated cotton	Acid yellow 99	–	448	–	Bouzaida and Rammah (2002)
Blast furnace sludge	Ethyl orange	28	1.3	–	Jain et al. (2003c)
Fly ash	Metomega chrome orange	–	0.743	10	Gupta and Shukla (1996)
Wollastonite	Metomega chrome orange	–	0.7	10	Gupta and Shukla (1996)
Kaolinite	Metomega chrome orange	–	0.65	10	Gupta and Shukla (1996)
Coal	Metomega chrome orange	–	0.77	10	Gupta and Shukla (1996)
Activated bentonite	Sella fast brown H	–	360.5	–	Espantaleon et al. (2003)

Reproduced from Gupta and Suhas (2009). With permission from Elsevier

Table 2.8 Adsorption capacities of commercial activated carbon and other alternative adsorbents for removal of basic dyes

Adsorbent	Adsorbate	Surface area of adsorbent (m_2/g)	Adsorption capacity (mg/g)	Concentration range (mg/L)	Source
Commercial AC (E. Merck India)	Basic blue 9 (methylene blue)		980.3	100–400	Kannan and Sundaram (2001)
CAC granular Wako (Wako Pure Chemicals)	Basic blue 9	1150	260	–	Okada et al. (2003)
CAC fiber FE400 (Toho Rayon Co.)	Basic blue 9	1010	170	–	Okada et al. (2003)
CAC felt KF1500 (Toyobo Co.)	Basic blue 9	1480	300	–	Okada et al. (2003)
Activated carbon	Basic blue 3	–	648.6	50–600	Nassar and Magdy (1997)
GAC (Miloje Zakic)	Basic dye Maxilon Goldgelb GL EC	–	159	20–200	Meshko et al. (2001)
GAC (Miloje Zakic)	Basic dye Maxilon Schwarz FBL-01	–	309.2	50–500	Meshko et al. (2001)
CAC Merck	Basic green 4 (malachite green)	765	222.22	–	Malik et al. (2007)
Chemviron F-400	Basic red 22	–	720	50–1000	Allen et al. (2003)
Activated carbon	Basic red 22	–	790	50–600	Nassar and Magdy (1997)
PAC Chemviron GW	Basic red 46	1026	106	30–250	Martin et al. (2003)
Chemviron F-400	Basic yellow 21	–	860	50–1000	Allen et al. (2003)
Activated carbon	Basic yellow 21	–	600	50–600	Nassar and Magdy (1997)
Activated sludge biomass	Basic blue 3	–	36.5	–	Chu and Chen (2002a)
Palm-fruit bunch (raw)	Basic blue 3	–	92	50–600	Nassar and Magdy (1997)
Activated sludge biomass	Basic blue 47	–	157.5	–	Chu and Chen (2002a)

Activated sludge biomass	Basic blue 54	–	86.6	–	Chu and Chen (2002a)
Carbonaceous adsorbent	Basic blue 6 (MeldolÃ¡s blue)	380	170	–	Jain et al. (2003b)
Blast furnace (BF) sludge, BF dust, BF slag	Basic blue 6 (MeldolÃ¡s blue)	28, 13, 4	67, 34, 3.7	–	Jain et al. (2003b)
AC-pinewood	Basic blue 69	902	1119	–	Tseng et al. (2003)
Bagasse pith raw	Basic blue 69	–	152	10–1000	Chen et al. (2001)
Wood sawdust (raw)	Basic blue 69	–	71.9	–	Ho and McKay (1998a)
Peat	Basic blue 69	–	195	–	Ho and McKay (1998b)
Wood	Basic blue 69 (Astrazone blue)	–	100.1	–	Poots et al. (1978)
Peat	Basic blue 69 (Astrazone blue)	–	40–910	200	McKay et al. (1981)
Hardwood sawdust	Basic blue 69 (Astrazone blue)	–	82.2–105.7	200	Asfour et al. (1985)
Activated clay	Basic blue 69, basic red 22	–	585, 488.4	–	El-Guendi et al. 1995
Bagasse pith	Basic blue 69, basic red 22	–	157.4, 76.6	200	McKay et al. (1997)
AC-pinewood	Basic blue 9	902	556	–	Tseng et al. (2003)
AC-waste newspaper	Basic blue 9	1740	390	–	Okada et al. (2003)
Bentonite	Basic blue 9 (methylene blue)	28	1667	100–1000	Ozacar and Sengil (2006)
Coal	Basic blue 9	–	250	10–1000	McKay et al. (1999)
Bark	Basic blue 9	–	914	10–1000	McKay et al. (1999)
Rice husk	Basic blue 9	–	312	10–1000	McKay et al. (1999)
Cotton waste	Basic blue 9	–	277	10–1000	McKay et al. (1999)
Hair	Basic blue 9	–	158	10–1000	McKay et al. (1999)

(continued)

Table 2.8 (continued)

Adsorbent	Adsorbate	Surface area of adsorbent (m_2/g)	Adsorption capacity (mg/g)	Concentration range (mg/L)	Source
Sewage sludge	Basic blue 9	–	114.94	–	Otero et al. (2003a)
Bamboo dust carbon	Basic blue 9	–	143.2	100–400	Kannan and Sundaram (2001)
Coconut shell carbon	Basic blue 9	–	277.9	100–400	Kannan and Sundaram (2001)
Groundnut shell carbon	Basic blue 9	–	164.9	100–400	Kannan and Sundaram (2001)
Rice husk carbon	Basic blue 9	–	343.5	100–400	Kannan and Sundaram (2001)
Straw carbon	Basic blue 9	–	472.1	100–400	Kannan and Sundaram (2001)
Raw date pits	Basic blue 9	–	80.3	20–400	Banat et al. (2003)
AC-apricot shell	Basic blue 9	783	4.11	–	Aygun et al. (2003)
AC-hazelnut shell	Basic blue 9	793	8.82	–	Aygun et al. (2003)
AC-walnut shell	Basic blue 9	774	3.53	–	Aygun et al. (2003)
Fly ash-Slovakia	Basic blue 9	3.26	1.47	16–64	Janos et al. (2003)
Fly ash-Czech Republic	Basic blue 9	5.47	6.04	16–64	Janos et al. (2003)
Fe(III)/Cr(III) hydroxide	Basic blue 9	–	22.8	–	Namasivayam and Sumithra (2005)
Banana peel (raw)	Basic blue 9	20.6–23.5	20.8	10–120	Annadurai et al. (2002)
Orange peel (raw)	Basic blue 9	20.6–23.5	18.6	–	Annadurai et al. (2002)
Clay	Basic blue 9	71	300	–	Bagane and Guiza (2000)
Diatomite	Basic blue 9	27.8	198	100–400	Al-Ghouti et al. (2003)
Diatomite	Basic blue 9	33	134	41–600	Shawabkeh and Tutunji (2003)

Clay	Basic blue 9	30	6.3	–	Gurses et al. (2004)
Activated sludge	Basic blue 9	–	256.41	–	Gulnaz et al. (2004)
Spirodela polyrrhiza biomass	Basic blue 9	–	144.93	–	Waranusantigul et al. (2003)
Dead fungus *Aspergillus niger*	Basic blue 9	–	10.49–18.54	50	Fu and Viraraghavan (2000)
Living biomass *Aspergillus niger*	Basic blue 9	–	1.17	50	Fu and Viraraghavan (2000)
Neem sawdust	Basic blue 9	–	3.622	12	Khattri and Singh (2000)
Yellow passion fruit	Basic blue 9	30	44.7	–	Pavan et al. (2008)
Guava leaf powder	Basic blue 9	–	295	100–800	Ponnusami et al. (2008)
Beer brewery waste	Basic blue 9	4.5	4.92	–	Tsai et al. (2008)
Jackfruit peel	Basic blue 9 (methylene blue)	–	285.713	35–400	Hameed (2009a)
Spent tea leaves	Basic blue 9 (methylene blue)	–	300.052	30–390	Hameed (2009b)
Sugarcane dust	Basic blue 9	–	3.745	12	Khattri and Singh (1999)
Carbonaceous adsorbent	Basic blue 9 (methylene blue)	380	92	–	Jain et al. (2003a)
Blast furnace (BF) sludge, BF dust, BF slag	Basic blue 9 (methylene blue)	28, 13, 4	6.4, 3.3, 2.1	–	Jain et al. (2003a)
Diatomite	Basic blue 9 (methylene blue)	27.8	198	100–400	Al-Ghouti et al. (2003)
Cedar sawdust, crushed brick	Basic blue 9 (methylene blue)	–	142.36, 96.41	–	Hamdaoui (2006)
Fly ash (treated with H_2SO_4)	Basic blue 9 (methylene blue)	6.236	0.67	8.5–85	Lin et al. (2008)

(continued)

Table 2.8 (continued)

Adsorbent	Adsorbate	Surface area of adsorbent (m_2/g)	Adsorption capacity (mg/g)	Concentration range (mg/L)	Source
Fly ash, zeolite, unburned carbon	Basic blue 9 (methylene blue)	15.6, 16.0, 224	6.4, 14.4, 80	0.32–3.2	Wang et al. (2005)
PET carbon	Basic blue 9 (methylene blue)	–	33.4	–	Zhang and Itoh (2003)
Hazelnut shell	Basic blue 9	–	76.9	50–1000, 50–500	Ferrero (2007)
Sawdust-walnut	Basic blue 9	–	59.17	50–1000, 50–500	Ferrero (2007)
Sawdust-cherry	Basic blue 9	–	39.84	50–1000, 50–500	Ferrero (2007)
Sawdust-oak	Basic blue 9	–	29.94	50–1000, 50–500	Ferrero (2007)
Sawdust-pitch pine	Basic blue 9	–	27.78	50–1000, 50–500	Ferrero (2007)
Sunflower stalk	Basic blue 9 (methylene blue), basic red 9	1.2054	205, 317	100–2000, 100–2000	Sun and Xu (1997)
Beech sawdust untreated	Basic blue 9 (methylene blue), red basic 22	–	9.78, 20.2	–	Batzias and Sidiras (2004)
Zeolite	Basic dye Maxilon Goldgelb GL EC	–	14.91	20–200	Meshko et al. (2001)
Zeolite	Basic dye Maxilon Schwarz FBL-01	–	55.86	50–500	Meshko et al. (2001)
Sawdust carbon	Basic green 4	–	74.5	50–250	Garg et al. (2003)
Neem sawdust	Basic green 4	–	3.42	12	Khattri and Singh (2000)
AC from pine sawdust	Basic green 4	1390	370.37	50–2000	Akmil-Basar et al. (2005)
Oil palm trunk fiber	Basic green 4 (malachite green)	–	149.35	25–300	Hameed and el-Khaiary (2008)
AC-groundnut shell	Basic green 4 (malachite green)	1114	222.22	–	Malik et al. (2007)

Waste material from paper industry, pine bark	Basic green 4 (malachite green)	–	–	100	Mendez et al. (2007)
Carbonaceous material	Basic green 4 (malachite green)	629	75.08	36.4–364	Gupta et al. (1997)
Sugarcane dust	Basic green 4 (malachite green)	–	3.999	12	Khattri and Singh (1999)
Carbonaceous adsorbent	Basic orange 2 (Chrysoidine G)	380	75	–	Jain et al. (2003b)
Blast furnace (BF) sludge, BF dust, BF slag	Basic orange 2 (Chrysoidine G)	28, 13, 4	10.1, 5.4, 1.9	–	Jain et al. (2003b)
Tree fern	Basic red 13	–	408	–	Ho et al. (2005)
Activated sludge	Basic red 18	–	285.71	–	Gulnaz et al. (2004)
Activated sludge biomass	Basic red 18	–	133.9	–	Chu and Chen (2002a)
Activated clay	Basic red 18 (C.I. 11,085)	–	157	–	Ho et al. (2001)
Coal	Basic red 2 (C.I. 50,240)	–	120	10–1000	McKay et al. (1999)
Bark	Basic red 2 (C.I. 50,240)	–	1119	10–1000	McKay et al. (1999)
Rice husk	Basic red 2 (C.I. 50,240)	–	838	10–1000	McKay et al. (1999)
Cotton waste	Basic red 2 (C.I. 50,240)	–	875	10–1000	McKay et al. (1999)
Human hair	Basic red 2 (C.I. 50,240)	–	190	10–1000	McKay et al. (1999)
Bentonite	Basic red 2 (C.I. 50,240)	47.73	274	50–450	Hu et al. (2006)
AC-plum kernel	Basic red 22	1162	710	–	Juang et al. (2002)
Sugar-industry-mud	Basic red 22	–	519	50–2000	Magdy and Daifullah (1998)
Kudzu	Basic red 22	–	210	50–1000	Allen et al. (2003)
Bagasse pith raw	Basic red 22	–	75	10–1000	Chen et al. (2001)
Palm-fruit bunch RAW	Basic red 22	–	180	50–600	Nassar and Magdy (1997)
AC-bagasse	Basic red 22 (C.I. 11,055)	607	942	–	Juang et al. (2002)

(continued)

Table 2.8 (continued)

Adsorbent	Adsorbate	Surface area of adsorbent (m_2/g)	Adsorption capacity (mg/g)	Concentration range (mg/L)	Source
Cane pith	Basic red 22 (C.I. 11,055)	606.8	941.7	–	Juang et al. (2001)
AC-corncob	Basic red 22 (C.I. 11,055)	943	790	–	Juang et al. (2002)
Activated sludge biomass	Basic red 29	–	113.2	–	Chu and Chen (2002a)
AC sludge based	Basic red 46	253	188	30–250	Martin et al. (2003)
Neem sawdust	Basic violet 10	–	2.355	12	Khattri and Singh (2000)
Fly ash-Slovakia	Basic violet 10	3.26	1.91	24–95.8	Janos et al. (2003)
Fly ash-Czech Republic	Basic violet 10	5.47	5.5	24–95.8	Janos et al. (2003)
Banana peel	Basic violet 10	20.6–23.5	20.6	10–120	Annadurai et al. (2002)
Orange peel	Basic violet 10	20.6–23.5	14.3	10–120	Annadurai et al. (2002)
Coir pith carbonized	Basic violet 10 (Rhodamine B)	259	2.56	–	Namasivayam et al. (2001)
Coir pith (raw)	Basic violet 10 (Rhodamine B)	–	203.25	–	Namasivayam et al. (2001)
Sugarcane dust	Basic violet 10 (Rhodamine B)	–	3.24	12	Khattri and Singh (1999)
Sewage sludge	Basic violet 14 (basic fuchsin)	–	70–127	10–1000	Seredych and Bandosz (2007)
Neem sawdust	Basic violet 3	–	3.789	12	Khattri and Singh (2000)
Activated sludge biomass	Basic violet 3	–	113.6	–	Chu and Chen (2002a)
Carbonaceous adsorbent	Basic violet 3 (crystal violet)	380	161	–	Jain et al. (2003b)
Blast furnace (BF) sludge, BF dust, BF slag	Basic violet 3 (crystal violet)	28, 13, 4	25, 11, 3	–	Jain et al. (2003b)
Activated sewage sludge	Basic violet 3 (crystal violet)	390	270.88	100–1000	Otero et al. (2003b)
Pyrolyzed sewage sludge	Basic violet 3 (crystal violet)	80	184.68	100–1000	Otero et al. (2003b)

Sugarcane dust	Basic violet 3 (crystal violet)	–	3.798	12	Khattri and Singh (1999)
Palm-fruit bunch (raw)	Basic yellow 21	–	327	50–600	Nassar and Magdy (1997)
Kudzu	Basic yellow 21	–	160	50–1000	Allen et al. (2003)
Activated sludge biomass	Basic yellow 24	–	105.6	–	Chu and Chen (2002b)

Reproduced from Gupta and Suhas (2009). With permission from Elsevier

Table 2.9 Adsorption capacities of commercial activated carbon and other alternative adsorbents for removal of dyes (apart from acid or basic dyes)

Adsorbent	Adsorbate	Surface area of adsorbent (m^2/g)	Adsorption capacity (mg/g)	Concentration range (mg/L)	Source
PAC Chemviron GW	Direct black 168	1026	18.7	30–250	Martin et al. (2003)
Filtrasorb 400 (Calgon Corporation)	Direct brown 1 (C.I. 30,110)	–	7.69	–	Venkata Mohan et al. (2002)
GAC Filtrasorb 400 (Calgon Corporation)	Direct red 28 (C.I. 22,120)	–	13.8	–	Fu and Viraraghavan (2002a)
PAC from Filtrasorb 400 (Calgon Corporation)	Direct red 28 (C.I. 22,120)	–	16.81	–	Fu and Viraraghavan (2002a)
PAC Chemviron GW	Direct red 89	1026	8.4	30–250	Martin et al. (2003)
CAC Aldrich	Reactive red X6BN Sandoz	–	163	25–1000	Oliveira et al. (2007)
Filtrasorb 400 (Chemviron Carbon UK)	Remazol golden yellow, Remazol red, Remazol black B	1100	1111, 400, 434	50–1000	Al-Degs et al. (2000)
AC sludge based	Direct black 168	253	28.9	30–250	Martin et al. (2003)
AC-orange peel	Direct blue 86	–	33.78	25–125	Nemr et al. (2009)
Charfines, lignite coal, bituminous coal	Direct brown (C.I. 30,110)	–	6.4, 4.1, 2.04	50	Venkata Mohan et al. (2002)
Banana pith	Direct red	–	5.92	–	Namasivayam et al. (1998)
Fe(III)/Cr(III) hydroxide	Direct red 12B	–	5	–	Namasivayam and Sumithra (2005)
Biogas residual slurry	Direct red 12B	–	3.46	–	Namasivayam and Yamuna (1995)
Orange peel	Direct red 23, direct red 80	–	10.72, 21.05	–	Arami et al. (2005)
Coir pith	Direct red 28	–	6.72	–	Namasivayam and Kavitha (2002)

Rice hull ash	Direct red 28	236.4	171	–	Chou et al. (2001)
Red mud	Direct red 28	–	4.05	–	Namasivayam and Arasi (1997)
Dead fungus *Aspergillus niger*	Direct red 28	–	14.16	–	Fu and Viraraghavan (2002a)
Banana peel	Direct red 28 (Congo red)	20.6–23.5	18.2	10–120	Annadurai et al. (2002)
Orange peel	Direct red 28 (Congo red)	20.6–23.5	14	10–120	Annadurai et al. (2002)
Activated red mud	Direct red 28 (Congo red)	–	7.08	10–90	Tor and Cengeloglu (2006)
Chitosan	Direct red 28 (Congo red)	–	81.23	–	Wang and Wang (2007)
Sunflower stalk	Direct red 28 (Congo red), direct blue	1.2054	37.78, 26.84	50–1000, 50–1000	Sun and Xu (1997)
Crude sewage sludge	Direct red 79	5.28	19.6	–	Dhaouadi and M'Henni (2008)
Mixture almond shells	Direct red 80	10.5	22.422	50–150	Doulati Ardejani et al. (2008)
Soy meal hull	Direct red 80, direct red 81	0.7623	178.57, 120.48	50–150	Arami et al. (2006)
Chitosan bead (chemically cross-linked)	Direct red 81	–	2383	–	Chiou et al. (2004)
AC sludge based	Direct red 89	253	49.2	30–250	Martin et al. (2003)
Powdered activated sludge	Direct yellow 12	–	98	–	Kargi and Ozmihci (2004)
Palm oil ash	Disperse blue, disperse red	–	49.5, 61.35	–	Hasnain Isa et al. (2007)
AC from biomass *Euphorbia rigida*	Disperse orange 25	741–21	118.93	50–125	Gercel et al. (2008)

(continued)

Table 2.9 (continued)

Adsorbent	Adsorbate	Surface area of adsorbent (m^2/g)	Adsorption capacity (mg/g)	Concentration range (mg/L)	Source
Modified fungal biomass (*Aspergillus niger*)	Disperse red 1 (C.I. 11,110)	–	5.59	13.5	Fu and Viraraghavan (2002b)
Modified sepiolite	Reactive black 5	50.5	120.5	–	Ozdemir et al. (2004)
Modified zeolite	Reactive black 5	11.8	60.5	–	Ozdemir et al. (2004)
Rhizopus arrhizus biomass	Reactive black 5	–	588.2	20–800	Aksu and Tezer (2000)
Sunflower seed shells, mandarin peelings	Reactive black 5	–	–	50	Osma et al. (2007)
High lime fly ash	Reactive black 5	5.35	7.184	5–100	Eren and Acar (2007)
Biomass *Chlorella vulgaris*	Reactive black B	–	555.6	20–800	Aksu and Tezer (2005)
Untreated alunite	Reactive blue 114 (C.I. 21,620)	–	2.92	–	Ozacar and Sengil (2003)
Calcined alunite	Reactive blue 114 (C.I. 21,620)	66	170.7	–	Ozacar and Sengil (2003)
Metal hydroxide sludge	Reactive blue 19	–	275	–	Santos et al. (2008)
Biomass *Rhizopus arrhizus*	Reactive blue 19 (C.I. 61,200)	–	90	0–500	O'Mahony et al. (2002)
Activated sludge	Reactive blue 2 (C.I. 61,211)	–	250	–	Aksu (2001)
Chitosan bead (chemically cross-linked)	Reactive blue 2, reactive red 2, reactive yellow 2, reactive yellow 86	–	2498, 2422, 2436, 1911	–	Chiou et al. (2004)
Charred dolomite	Reactive dye Levafix brilliant red E-4BA	36	950	100–2000	Walker et al. (2003)
Squid pens	Reactive green 12, direct green 26	8.82	39.8, 4.83	–	Figueiredo et al. (2000)

Sepia pens	Reactive green 12, direct green 26	4.11	3.46, 56.0	–	Figueiredo et al. (2000)
Anodonta shell	Reactive green 12, direct green 26	1.42	0.436, 11.3	–	Figueiredo et al. (2000)
Biomass *Rhizopus arrhizus*	Reactive orange 16 (C.I. 17,757)	–	190	0–500	O'Mahony et al. (2002)
Metal hydroxide sludge	Reactive red 120	–	48.31	10–200	Netpradit et al. (2003)
Untreated alunite	Reactive red 124 (C.I. 17,780)	–	2.85	–	Ozacar and Sengil (2003)
Calcined alunite	Reactive red 124 (C.I. 17,780)	66	153	–	Ozacar and Sengil (2003)
Metal hydroxide sludge	Reactive red 141	–	56.18	10–200	Netpradit et al. (2003)
Cross-linked chitosan bead	Reactive red 189	–	1936	–	Chiou and li (2002)
Non-cross-linked chitosan bead	Reactive red 189	–	1189	–	Chiou and li (2002)
Metal hydroxide sludge	Reactive red 2	–	62.5	10–200	Netpradit et al. (2003)
Chitosan bead (crab)	Reactive red 222	–	1106	–	Wu et al. (2000)
Chitosan bead (lobster)	Reactive red 222	–	1037	–	Wu et al. (2000)
Chitosan bead (shrimp)	Reactive red 222	–	1026	–	Wu et al. (2000)
Chitosan flake (shrimp)	Reactive red 222	–	494	–	Wu et al. (2000)
Chitosan flake (crab)	Reactive red 222	–	293	–	Wu et al. (2000)
Modified sepiolite	Reactive red 239	50.5	108.8	–	Ozdemir et al. (2004)
Modified zeolite	Reactive red 239	11.8	111.1	–	Ozdemir et al. (2004)
Biomass *Rhizopus arrhizus*	Reactive red 4 (C.I. 18,105)	–	150	0–500	O'Mahony et al. (2002)

(continued)

Table 2.9 (continued)

Adsorbent	Adsorbate	Surface area of adsorbent (m^2/g)	Adsorption capacity (mg/g)	Concentration range (mg/L)	Source
Chromium-containing leather waste	Reactive red X6BN Sandoz	–	48	25–1000	Oliveira et al. (2007)
Modified sepiolite	Reactive yellow 176	50.5	169.1	–	Ozdemir et al. (2004)
Modified zeolite	Reactive yellow 176	11.8	88.5	–	Ozdemir et al. (2004)
Activated sludge	Reactive yellow 2 (CI 18972)	–	333.3	–	Aksu (2001)
Treated cotton	Reactive yellow 23	–	302	–	Bouzaida and Rammah (2002)
Untreated alunite	Reactive yellow 64 (C.I. 29,025)	–	5	–	Ozacar and Sengil (2003)
Calcined alunite	Reactive yellow 64 (C.I. 29,025)	66	236	–	Ozacar and Sengil (2003)
Eucalyptus bark	Remazol BB	–	90	500	Morais et al. (1999)
Yeast (*Saccharomyces cerevisiae*)	Remazol black B	–	88.5	10–400	Aksu (2003)
Yeast (*Saccharomyces cerevisiae*)	Remazol blue	–	84.6	10–400	Aksu (2003)
Yeast-*C. lipolytica*	Remazol blue	–	250	100–400	Aksu and Donmez (2003)
Yeast-*C. tropicalis*	Remazol blue	–	182	100–400	Aksu and Donmez (2003)
Yeast-*Candida* sp.	Remazol blue	–	167	100–400	Aksu and Donmez (2003)
Yeast-*C. quilliermendii*	Remazol blue	–	154	100–400	Aksu and Donmez (2003)
Yeast-*C. utilis*	Remazol blue	–	114	100–400	Aksu and Donmez (2003)

Biomass *Chlorella vulgaris*	Remazol golden-yellow RNL	–	71.9	10–200	Aksu and Tezer (2005)
Yeast (*Saccharomyces cerevisiae*)	Remazol red RB	–	48.8	10–400	Aksu (2003)
Biomass *Chlorella vulgaris*	Remazol red RR	–	196.1	20–800	Aksu and Tezer (2005)
Crude sewage sludge	Vat blue 4	5.28	248.3	–	Dhaouadi and M'Henni (2008)

Reproduced from Gupta and Suhas (2009). With permission from Elsevier

References

Akmil-Basar C, Onal Y, Kilicer T, Eren D (2005) Adsorptions of high concentration malachite green by two activated carbons having different porous structures. J Hazard Mater 127:73–80
Aksu Z (2001) Biosorption of reactive dyes by dried activated sludge: equilibrium and kinetic modelling. Biochem Eng J 7:79–84
Aksu Z (2003) Reactive dye bioaccumulation by Saccharomyces cerevisiae. Process Biochem 38:1437–1444
Aksu Z, Donmez G (2003) A comparative study on the biosorption characteristics of some yeasts for Remazol blue reactive dye. Chemosphere 50:1075–1083
Aksu Z, Tezer S (2000) Equilibrium and kinetic modelling of biosorption of Remazol black B by Rhizopus arrhizus in a batch system: effect of temperature. Process Biochem 36:431–439
Aksu Z, Tezer S (2005) Biosorption of reactive dyes on the green alga Chlorella Vulgaris. Process Biochem 40:1347–1361
Al-Degs Y, Khraisheh MAM, Allen SJ, Ahmad MN (2000) Effect of carbon surface chemistry on the removal of reactive dyes from textile effluent. Water Res 34:927–935
Al-Ghouti MA, Khraisheh MAM, Allen SJ, Ahmad MN (2003) The removal of dyes from textile wastewater: a study of the physical characteristics and adsorption mechanisms of diatomaceous earth. J Environ Manag 69:229–238
Allen SJ, Gan Q, Matthews R, Johnson PA (2003) Comparison of optimized isotherm models for basic dye adsorption by kudzu. Bioresour Technol 88:143–152
Annadurai G, Juang RS, Lee DJ (2002) Use of cellulose-based wastes for adsorption of dyes from aqueous solutions. J Hazard Mater 92:263–274
Arami M, Limaee NY, Mahmoodi NM, Tabrizi NS (2006) Equilibrium and kinetics studies for the adsorption of direct and acid dyes from aqueous solution by soy meal hull. J Hazard Mater 135:171–179
Asfour HM, Fadali OA, Nassar MM, EI-Geundi MS (1985) Equilibrium studies on adsorption of basic dyes on hardwood. J Chem Technol Biotechnol 35A:21–27
Aygun A, Yenisoy-Karakas S, Duman I (2003) Production of granular activated carbon from fruit stones and nutshells and evaluation of their physical, chemical and adsorption properties. Microporous Mesoporous Mater 66:189–195
Bagane M, Guiza S (2000) Elimination d'un colorant des effluents de l'industrie textile par adsorption. Ann Chim Sci Mater 25:615–625
Banat F, Al-Asheh S, Al-Makhadmeh L (2003) Evaluation of the use of raw and activated date pits as potential adsorbents for dye containing waters. Process Biochem 39:193–202
Batzias FA, Sidiras DK (2004) Dye adsorption by calcium chloride treated beech sawdust in batch and fixed-bed systems. J Hazard Mater 114:167–174
Bhattacharyya KG, Sarma A (2003) Adsorption characteristics of the dye, Brilliant Green, on Neem leaf powder. Dyes Pigm 57(3):211–222
Bohart G, Adams EQ (1920) Some aspects of the behavior of charcoal with respect to chlorine. J Am Chem Soc 42:523–544
Bouzaida I, Rammah MB (2002) Adsorption of acid dyes on treated cotton in a continuous system. Mater Sci Eng C 21:151–155
Chatzopoulos D, Verma A, Irvine RL (1993) Activated carbon adsorption and desorption of toluene in the aqueous phase. AICHE J 39:2027–2041
Chen BN, Hui CW, McKay G (2001) Film-pore diffusion modeling and contact time optimization for the adsorption of dyestuffs on pith. Chem Eng J 84:77–94
Chiou MS, Li HY (2002) Equilibrium and kinetic modeling of adsorption of reactive dye on cross-linked chitosan beads. J Hazard Mater 93:233–248
Chiou MS, Ho PY, Li HY (2004) Adsorption of anionic dyes in acid solutions using chemically cross-linked chitosan beads. Dyes Pigments 60:69–84
Choy KKH, McKay G, Porter JF (1999) Sorption of acid dyes from effluents using activated carbon. Resour Conserv Recycl 27:57–71

Choy KKH, Porter JF, McKay G (2000) Langmuir isotherm models applied to the multicomponent sorption of acid dyes from effluent onto activated carbon. J Chem Eng Data 45:575–584
Chu HC, Chen KM (2002a) Reuse of activated sludge biomass: I. Removal of basic dyes from wastewater by biomass. Process Biochem 37:595–600
Chu HC, Chen KM (2002b) Reuse of activated sludge biomass: II. The rate processes for the adsorption of basic dyes on biomass. Process Biochem 37:1129–1134
Clark RM (1987) Evaluating the cost and performance of field-scale granular activated carbon systems. Environ Sci Technol 21:573–580
Costa E, Calleja G, Marijuan L (1987) Adsorption of phenol and p-nitrophenol on activated carbon: determination of effective diffusion coefficient. Adsorp Sci Technol 4:59–77
Dedrick RL, Beckmann RB (1967) Kinetics of adsorption by activated carbon from dilute aqueous solution. AIChe Symp Ser 63:68–78
Dhaouadi H, M'Henni F (2008) Textile mill effluent decolorization using crude dehydrated sewage sludge. Chem Eng J 138:111–119
Doulati Ardejani F, Badii K, Limaee NY, Shafaei SZ, Mirhabibi AR (2008) Adsorption of direct red 80 dye from aqueous solution onto almond shells: effect of pH, initial concentration and shell type. J Hazard Mater 151:730–737
El-Guendi MS, Ismail HM, Attyia KME (1995) Activated clay as an adsorbent for cationic dyestuffs. Adsorpt Sci Technol 12:109–117
Eren Z, Acar FN (2007) Equilibrium and kinetic mechanism for reactive black 5 sorption onto high lime Soma fly ash. J Hazard Mater 143:226–232
Espantaleon AG, Nieto JA, Fernandez M, Marsal A (2003) Use of activated clays in the removal of dyes and surfactants from tannery waste waters. Appl Clay Sci 24:105–111
Faust SD, Aly OM (1987) Adsorption processes for water treatment. Butterworth Publishers, USA
Ferrero F (2007) Dye removal by low cost adsorbents: hazelnut shells in comparison with wood sawdust. J Hazard Mater 142:144–152
Figueiredo SA, Boaventura RA, Loureiro JM (2000) Color removal with natural adsorbents: modeling, simulation and experimental. Sep Purif Technol 20:129–141
Finar IL (1973) Addison Wesley Longman ltd., organic chemistry, Vol-1: the fundamental principles
Fogler HS (1997) Elements of chemical reaction engineering. Prentice Hall (India) Ltd, New Delhi
Fu YZ, Viraraghavan T (2000) Removal of a dye from an aqueous solution by the fungus Aspergillus niger. Water Qual Res J Can 35:95–111
Fu YZ, Viraraghavan T (2001) Removal of CI acid blue 29 from an aqueous solution by Aspergillus niger. Am Assoc Text Chem Color Rev 1:36–40
Fu Y, Viraraghavan T (2002a) Removal of Congo Red from an aqueous solution by fungus Aspergillus niger. Adv Environ Res 7:239–247
Fu YZ, Viraraghavan T (2002b) Dye biosorption sites in Aspergillus niger. Bioresour Technol 82:139–145
Furusawa T, Smith JM (1973) Fluid-particle and intraparticle mass transport rates in slurries. Ind Eng Chem Fundamen 12:197–203
Garg VK, Gupta R, Bala Yadav A, Kumar R (2003) Dye removal from aqueous solution by adsorption on treated sawdust. Bioresour Technol 89:121–124
Gercel O, Gercel HF, Koparal AS, Ogutveren UB (2008) Removal of disperse dye from aqueous solution by novel adsorbent prepared from biomass plant material. J Hazard Mater 160:668–674
Goel J, Kadirvelu K, Rajagopal C, Garg VK (2005) Removal of lead(II) by adsorption using treated granular activated carbon: batch and column studies. J Hazard Mater 125:211–220
Gulnaz O, Kaya A, Matyar F, Arikan B (2004) Sorption of basic dyes from aqueous solution by activated sludge. J Hazard Mater 108:183–188
Gupta GS, Shukla SP (1996) An inexpensive adsorption technique for the treatment of carpet effluents by low cost materials. Adsorp Sci Technol 13:15–26

Gupta VK, Suhas (2009) Application of low cost adsorbents for dye removal – a review. J Environ Manage 90:2313–2342
Gupta VK, Srivastava SK, Mohan D (1997) Equilibrium uptake, sorption dynamics, process optimization, and column operations for the removal and recovery of malachite green from wastewater using activated carbon and activated slag. Ind Eng Chem Res 36:2207–2218
Gupta VK, Mohan D, Sharma S, Sharma M (2000) Removal of basic dyes (Rhodamine B and Methylene Blue) from aqueous solutions using bagasse fly ash. Sep Sci Technol 35:2097–2113
Gupta VK, Mittal A, Kurup L, Mittal J (2006) Adsorption of a hazardous dye, erythrosine, over hen feathers. J Colloid Interface Sci 304:52–57
Gupta VK, Carrott PJM, Carrott R, Suhas MML (2009) Low cost adsorbents: growing approach to wastewater treatment – a review. Crit Rev Env Sci Technol 39:783–842
Gurses A, Karaca S, Dogar C, Bayrak R, Acikyildiz M, Yalcin M (2004) Determination of adsorptive properties of clay/water system: methylene blue sorption. J Colloid Interface Sci 269:310–314
Hamdaoui O (2006) Batch study of liquid-phase adsorption of methylene blue using cedar sawdust and crushed brick. J Hazard Mater 135:264–273
Hameed BH (2009a) Removal of cationic dye from aqueous solution using jackfruit peel as non-conventional low-cost adsorbent. J Hazard Mater 162:344–350
Hameed BH (2009b) Spent tea leaves: a new non-conventional and low-cost adsorbent for removal of basic dye from aqueous solutions. J Hazard Mater 161:753–759
Hameed BH, El-Khaiary MI (2008) Batch removal of malachite green from aqueous solutions by adsorption on oil palm trunk fibre: equilibrium isotherms and kinetic studies. J Hazard Mater 154:237–244
Hand DW, Crittenden JE, Thacker WE (1983) User oriented batch reactor solutions to the homogeneous surface diffusion model. J Environ Eng 109:82–101
Hasnain Isa M, Siew Lang L, Asaari FAH, Aziz HA, Azam Ramli N, Dhas JPA (2007) Low cost removal of disperse dyes from aqueous solution using palm ash. Dyes Pigments 74:446–453
Ho YS, McKay G (1998a) Kinetic models for the sorption of dye from aqueous solution by wood. Process Saf Environ Prot 76:183–191
Ho YS, McKay G (1998b) Sorption of dye from aqueous solution by peat. Chem Eng J 70:115–124
Ho YS, Wase DAJ, Forster CF (1996) Kinetic studies of competitive heavy metal adsorption by sphagnum moss peat. Environ Technol 17:71–77
Ho YS, Chiang TH, Hsueh YM (2005) Removal of basic dye from aqueous solution using tree fern as a biosorbent. Process Biochem 40:119–124
Hu QH, Qiao SZ, Haghseresht F, Wilson MA, Lu GQ (2006) Adsorption study for removal of basic red dye using bentonite. Ind Eng Chem Res 45:733–738
Jain AK, Gupta VK, Bhatnagar A, Jain S, Suhas (2003a) A comparative assessment of adsorbents prepared from industrial wastes for the removal of cationic dye. J Indian Chem Soc 80:267–270
Jain AK, Gupta VK, Bhatnagar A, Suhas (2003b) A comparative study of adsorbents prepared from industrial wastes for removal of dyes. Sep Sci Technol 38:463–481
Jain AK, Gupta VK, Bhatnagar A, Suhas (2003c) Utilization of industrial waste products as adsorbents for the removal of dyes. J Hazard Mater 101:31–42
Janos P, Buchtova H, Ryznarova M (2003) Sorption of dyes from aqueous solutions onto fly ash. Water Res 37:4938–4944
Juang RS, Tseng RL, Wu FC (2001) Role of microporosity of activated carbons on their adsorption abilities for phenols and dyes. Adsorption 7:65–72
Juang RS, Wu FC, Tseng RL (2002) Characterization and use of activated carbons prepared from bagasses for liquid-phase adsorption. Colloids Surf A Physicochem Eng Asp 201:191–199
Kannan N, Sundaram MM (2001) Kinetics and mechanism of removal of methylene blue by adsorption on various carbons – a comparative study. Dyes Pigments 51:25–40
Kapoor A, Yang RT, Wong C (1989) Surface diffusion. Catal Rev Sci Eng 31:129–214

Kargi F, Ozmihci S (2004) Biosorption performance of powdered activated sludge for removal of different dyestuffs. Enzym Microb Technol 35:267–271
Khan SA, Rehma R, Khan MM (1995) Adsorption of Cr(III), Cr(VI) and Ag(I) on Bentonite. Waste Manag 15:271–282
Khattri SD, Singh MK (1999) Colour removal from dye wastewater using sugar cane dust as an adsorbent. Adsorpt Sci Technol 17:269–282
Khattri SD, Singh MK (2000) Colour removal from synthetic dye wastewater using a bioadsorbent. Water Air Soil Pollut 120:283–294
Komiyama H, Smith J (1974) Surface diffusion in liquid filled pores. AICHE J 20:1110–1117
Kunii D, Levenspiel O (1991) Fluidization engineering. Butterworth-Heinemann, Oxford
Levenspiel O (1972) Chemical reaction engineering. Wiley, New York
Liapis AI, Rippin DWT (1977) A general model for the simulation of multicomponent adsorption from a finite batch. Chem Eng Sci 23:619–629
Lin JX, Zhan SL, Fang MH, Qian XQ, Yang H (2008) Adsorption of basic dye from aqueous solution onto fly ash. J Environ Manag 87:193–200
Magdy YH, Daifullah AAM (1998) Adsorption of a basic dye from aqueous solutions onto sugar-industry-mud in two modes of operations. Waste Manag 18:219–226
Malik PK (2003) Use of activated carbons prepared from sawdust and rice-husk for adsorption of acid dyes: a case study of acid yellow 36. Dyes Pigments 56:239–249
Malik R, Ramteke DS, Wate SR (2007) Adsorption of malachite green on groundnut shell waste based powdered activated carbon. Waste Manag 27:1129–1138
Manju GN, Raji C, Anirudhan TS (1998) Evaluation of coconut husk carbon for the removal of arsenic from water. Water Res 32:3062–3070
Martel B, Devassine M, Crini G, Weltrowski M, Bourdonneau M, Morcellet M (2001) Preparation and sorption properties of a beta-cyclodextrin-linked chitosan derivative. J Polym Sci Part A: Polym Chem 39:169–176
Martin MJ, Artola A, Balaguer MD, Rigola M (2003) Activated carbons developed from surplus sewage sludge for the removal of dyes from dilute aqueous solutions. Chem Eng J 94:231–239
Mathews P, Weber WJ Jr (1976) Effects of external mass transfer and intraparticle diffusion on adsorption rates in slurry reactors. AIChe Symp Ser 73
McKay G (1984) Analytical solution using a pore diffusion model for a pseudoirreversible isotherm for the adsorption of basic dye on silica. AIChE J 30(4):692–697
McKay G, Allen SJ, McConvey IF, Otterburn MS (1981) Transport processes in the sorption of colored ions by peat particles. J Colloid Interface Sci 80:323–339
McKay G, El-Geundi M, Nassar MM (1997) Equilibrium studies for the adsorption of dyes on bagasse pith. Adsorpt Sci Technol 15:251–270
McKay G, Porter JF, Prasad GR (1999) The removal of dye colours from aqueous solutions by adsorption on low-cost materials. Water Air Soil Pollut 114:423–438
Mendez A, Fernandez F, Gasco G (2007) Removal of malachite green using carbon-based adsorbents. Desalination 206:147–153
Meshko V, Markovska L, Mincheva M, Rodrigues AE (2001) Adsorption of basic dyes on granular activated carbon and natural zeolite. Water Res 35:3357–3366
Mohamed MM (2004) Acid dye removal: comparison of surfactant-modified mesoporous FSM-16 with activated carbon derived from rice husk. J Colloid Interface Sci 272:28–34
Morais LC, Freitas OM, Goncalves EP, Vasconcelos LT, Gonzalez Beca CG (1999) Reactive dyes removal from wastewaters by adsorption on eucalyptus bark: variables that define the process. Water Res 33:979–988
Motoyuki S (1990) Adsorption engineering. Elsevier Science Publishers, Tokyo
Namasivayam C, Arasi D (1997) Removal of Congo Red from wastewater by adsorption onto waste red mud. Chemosphere 34:401–417
Namasivayam C, Kavitha D (2002) Removal of Congo Red from water by adsorption onto activated carbon prepared from coir pith, an agricultural solid waste. Dyes Pigments 54:47–58

Namasivayam C, Sumithra S (2005) Removal of direct red 12B and methylene blue from water by adsorption onto Fe (III)/Cr(III) hydroxide, an industrial solid waste. J Environ Manag 74:207–215
Namasivayam C, Yamuna RT (1995) Adsorption of direct red 12B by biogas residual slurry equilibrium and rate processes. Environ Pollut 89:1–7
Namasivayam C, Prabha D, Kumutha M (1998) Removal of direct red and acid brilliant blue by adsorption on to banana pith. Bioresour Technol 64:77–79
Namasivayam C, Dinesh Kumar M, Selvi K, Ashruffunissa Begum R, Vanathi T, Yamuna RT (2001) 'Waste' coir pith–a potential biomass for the treatment of dyeing wastewaters. Biomass Bioenergy 21:477–483
Nassar MM, Magdy YH (1997) Removal of different basic dyes from aqueous solutions by adsorption on palm-fruit bunch particles. Chem Eng J 66:223–226
Nemr AE, Abdelwahab O, El-Sikaily A, Khaled A (2009) Removal of direct blue- 86 from aqueous solution by new activated carbon developed from orange peel. J Hazard Mater 161:102–110
Neretnieks I (1976) Adsorption in finite batch and counter flow with systems having a nonlinear isotherm. Chem Eng Sci 31:107–114
Netpradit S, Thiravetyan P, Towprayoon S (2003) Application of 'waste' metal hydroxide sludge for adsorption of azo reactive dyes. Water Res 37:763–772
O'Mahony T, Guibal E, Tobin JM (2002) Reactive dye biosorption by Rhizopus arrhizus biomass. Enzym Microb Technol 31:456–463
Okada K, Yamamoto N, Kameshima Y, Yasumori A (2003) Adsorption properties of activated carbon from waste newspaper prepared by chemical and physical activation. J Colloid Interface Sci 262:194–199
Oliveira LCA, Goncalves M, Oliveira DQL, Guerreiro MC, Guilherme LRG, Dallago RM (2007) Solid waste from leather industry as adsorbent of organic dyes in aqueous-medium. J Hazard Mater 141:344–347
Osma JF, Saravia V, Toca-Herrera JL, Couto SR (2007) Sunflower seed shells: a novel and effective low-cost adsorbent for the removal of the diazo dye Reactive Black 5 from aqueous solutions. J Hazard Mater 147:900–905
Otero M, Rozada F, Calvo LF, Garcia AI, Moran A (2003a) Kinetic and equilibrium modelling of the methylene blue removal from solution by adsorbent materials produced from sewage sludges. Biochem Eng J 15:59–68
Otero M, Rozada F, Calvo LF, Garcıá AI, Morań A (2003b) Elimination of organic water pollutants using adsorbents obtained from sewage sludge. Dyes Pigments 57:55–65
Ozacar M, Sengil IA (2002) Adsorption of acid dyes from aqueous solutions by calcined alunite and granular activated carbon. Adsorption 8:301–308
Ozacar M, Sengil IA (2003) Adsorption of reactive dyes on calcined alunite from aqueous solutions. J Hazard Mater B98:211–224
Ozacar M, Sengil IA (2005) Adsorption of metal complex dyes from aqueous solutions by pine sawdust. Bioresour Technol 96:791–795
Ozacar M, Sengil IA (2006) A two stage batch adsorber design for methylene blue removal to minimize contact time. J Environ Manag 80:372–379
Ozcan AS, Erdem B, Ozcan A (2004) Adsorption of acid blue 193 from aqueous solutions onto Na-bentonite and DTMA-bentonite. J Colloid Interface Sci 280:44–54
Ozdemir O, Armagan B, Turan M, Celik MS (2004) Comparison of the adsorption characteristics of azo-reactive dyes on mezoporous minerals. Dyes Pigments 62:49–60
Pavan FA, Lima EC, Dias SLP, Mazzocato AC (2008) Methylene blue biosorption from aqueous solutions by yellow passion fruit waste. J Hazard Mater 150:703–712
Ponnusami V, Vikram S, Srivastava SN (2008) Guava (Psidium Guajava) leaf powder: novel adsorbent for removal of methylene blue from aqueous solutions. J Hazard Mater 152:276–286
Poots VJP, McKay G, Healy JJ (1976a) The removal of acid dye from effluent using natural adsorbents—I peat. Water Res 10:1061–1066

Poots VJP, McKay G, Healy JJ (1976b) The removal of acid dye from effluent using natural adsorbents – II wood. Water Res 10:1067–1070
Poots VJP, McKay G, Healy JJ (1978) Removal of basic dye from effluent using wood as an adsorbent. J Water Pollut Control Fed 50:926
Purkait MK, Gusain DS, Dasgupta S, De S (2004) Adsorption behavior of Chrysoidine dye on activated Charcoal and its regeneration characteristics by using different surfactants. Sep Sci Technol 39:2419–2440
Purkait MK, Dasgupta S, De S (2005) Adsorption of eosin dye on activated carbon and its surfactant based desorption. J Environ Manage 76:135–142
Purkait MK, Maiti A, Dasgupta S, De S (2007) Removal of congo red using activated carbon and its regeneration. J Hazard Mater 145:287–295
Santos SCR, Vilar VJP, Boaventura RAR (2008) Waste metal hydroxide sludge as adsorbent for a reactive dye. J Hazard Mater 153:999–1008
Sekaran G, Shanmughasundaram KA, Mariaappan M, Raghavan KV (1995) Utilisation of a solid waste generated in leather industry for removal of dye in aqueous solution. Indian J Chem Technol 2:311–316
Seredych M, Bandosz TJ (2007) Removal of cationic and ionic dyes on industrial-municipal sludge based composite adsorbents. Ind Eng Chem Res 46:1786–1793
Shawabkeh RA, Tutunji MF (2003) Experimental study and modeling of basic dye sorption by diatomaceous clay. Appl Clay Sci 24:111–120
Singha S, Sarkar U, Mondal S, Saha S (2012) Transient behavior of a packed column of Eichhornia Crassipes stem for the removal of hexavalent chromium. Desalination 297:48–58
Sivaraj R, Namasivayam C, Kadirvelu K (2001) Orange peel as an adsorbent in the removal of acid violet 17 (acid dye) from aqueous solutions. Waste Manag 21:105–110
Spahn H, Schlunder EU (1975) the scale-up of activated carbon columns for water purification, based on results from batch tests—I: theoretical and experimental determination of adsorption rates of single organic solutes in batch tests. Chem Eng Sci 30:529–537
Sun G, Xu X (1997) Sunflower stalk as adsorbents for color removal from textile wastewater. Ind Eng Chem Res 36:808–812
Thinakaran N, Panneerselvam P, Baskaralingam P, Elango D, Sivanesan S (2008) Equilibrium and kinetic studies on the removal of acid red 114 from aqueous solutions using activated carbons prepared from seed shells. J Hazard Mater 158:142–150
Thomas HC (1944) Heterogeneous ion exchange in a flowing system. J Am Chem Soc 66:1664–1466
Tor A, Cengeloglu Y (2006) Removal of congo red from aqueous solution by adsorption onto acid activated red mud. J Hazard Mater 138:409–415
Tsai WT, Hsu HC, Su TY, Lin KY, Lin CM (2008) Removal of basic dye (methylene blue) from wastewaters utilizing beer brewery waste. J Hazard Mater 154:73–78
Tseng RL, Wu FC, Juang RS (2003) Liquid-phase adsorption of dyes and phenols using pinewood-based activated carbons. Carbon 41:487–495
Valix M, Cheung WH, McKay G (2004) Preparation of activated carbon using low temperature carbonisation and physical activation of high ash raw bagasse for acid dye adsorption. Chemosphere 56:493–501
Venkata Mohan S, Sailaja P, Srimurali M, Karthikeyan J (1999) Colour removal of monoazo acid dye from aqueous solution by adsorption and chemical coagulation. Environ Eng Policy 1:149–154
Walker GM, Hansen L, Hanna JA, Allen SJ (2003) Kinetics of a reactive dye adsorption onto dolomitic sorbents. Water Res 37:2081–2089
Wang L, Wang A (2007) Adsorption characteristics of Congo red onto the chitosan/montmorillonite nanocomposite. J Hazard Mater 147:979–985
Wang S, Li L, Wu H, Zhu ZH (2005) Unburned carbon as a low-cost adsorbent for treatment of methylene blue-containing wastewater. J Colloid Interface Sci 292:336–343

Waranusantigul P, Pokethitiyook P, Kruatrachue M, Upatham ES (2003) Kinetics of basic dye (methylene blue) biosorption by giant duckweed (Spirodela polyrrhiza). Environ Pollut 125:385–392

Weber WJ Jr, Rumer RR Jr (1965) Intraparticle transport of sulfonated alkylbenzenes in a porous solid: diffusion and non-linear adsorption. Water Resour Res 1:361–373

Wong YC, Szeto YS, Cheung WH, McKay G (2004) Adsorption of acid dyes on chitosan–equilibrium isotherm analyses. Process Biochem 39:695–704

Wu FC, Tseng RL, Juang RS (2000) Comparative adsorption of metal and dye on flake- and bead-types of chitosans prepared from fishery wastes. J Hazard Mater 73:63–75

Yoon YH, Nelson JH (1984) Application of gas adsorption kinetics. I. A theoretical model for respirator cartridge service time. Am Ind Hyg Assoc J 45:509–516

Zhang FS, Itoh H (2003) Adsorbents made from waste ashes and post-consumer PET and their potential utilization in wastewater treatment. J Hazard Mater 101:323–337